8-2021

The Facility Infection Risk Estimator™: A Web Application Tool for Comparing Indoor Risk Mitigation Strategies by Estimating Airborne Transmission Risk

Marcel Harmon
BranchPattern, harmon.m@branchpattern.com

Josephine Lau
University of Nebraska - Lincoln, jlau3@unl.ed

Title: The Facility Infection Risk Estimator™: A web application tool for comparing indoor risk mitigation strategies by estimating airborne transmission risk

Marcel Harmon, PhD, PE, WELL AP, LEED AP O+M
Associate Principal
BranchPattern
7400 College Boulevard, Suite 150, Overland Park, KS 66210
913-254-3427
marcel.h@branchpattern.com
https://branchpattern.com/

Josephine Lau, PhD
Associate Professor of Durham School of Architectural Engineering and Construction
College of Engineering
University of Nebraska–Lincoln
105D Peter Kiewit Institute, 1110 South 67th Street, Omaha, NE 68182-0681
402-554-2079
jlau3@unl.edu
http://engineering.unl.edu/durhamschool/faculty/josephine-lau/

Corresponding author email address: marcel.h@branchpattern.com

Abstract

The COVID-19 pandemic created needs for a) estimating the existing airborne risk of infection from SARS-CoV-2 in existing facilities and new designs, and b) estimating and comparing the impacts of engineering and behavioural strategies for contextually reducing that risk. This paper presents the development of a web application to meet these needs, the Facility Infection Risk Estimator™,[1] and its underlying Wells-Riley based model. The model specifically estimates a) the removal efficiencies of various settling, ventilation, filtration, and virus inactivation strategies and b) the associated probability of infection given the room physical parameters and number of individuals infected present with either influenza or SARS-CoV-2. A review of the underlying calculations and associated literature is provided, along with the model's validation against two documented spreading events. The error between modelled and actual number of additional people infected, normalized by the number of uninfected people present, ranged from roughly -18.4% to +9.7%. The more certain one can be regarding the input parameters (such as for new designs or existing buildings with adequate field verification), the smaller these normalized errors will be, likely less than ±15%, making it useful for comparing the impacts of different risk mitigation strategies focused on airborne transmission.

Keywords

infection risk; Wells-Riley; airborne transmission; influenza; SARS-CoV-2

Introduction

At the beginning of the pandemic in early 2020, there was an expressed need from various building owners, facility managers, occupants, and AEC industry consultants to help evaluate the relative contribution of different interior COVID-19 risk mitigation strategies. There was a lack of easily accessible tools and other resources for comparing and ranking different engineering / behavioural strategies (e.g., increased ventilation, filtration, mask wearing, de-densifying, germicidal UV technologies, etc.) for a given context based on both a) removal efficiency and b) the probability of infection. The model presented in this paper and its web-based application[1] were developed specifically to contextually compare and rank available influenza and SARS-CoV-2 mitigation strategies for making any built environment safer with respect to far-field virus-containing aerosols. Other modes of transmission exist with varying degrees of relevance for different pathogens, such as fomite or direct physical contact. Additional risk mitigation strategies are associated with these other modes of transmission, such as surface cleaning, which are not included in this model. However, the consensus among many scientists at this point is that the dominant route of transmission of SARS-CoV-2 is airborne.[2] There is increasing evidence that this also applies to Influenza and other respiratory viruses,[3,4,5] further indicating a need for tools capable of evaluating the risk mitigation potential relative to airborne transmission.

Airborne in this case refers to the transmission of viral particles or other pathogens from an infected individual through the air to an uninfected individual who inhales a quantity of particles sufficient to result in infection. Aerosols expelled from the infected individual act as the transport “vehicles” for the pathogens and depending on their size and environmental conditions, may float in the air for hours or even days. Aerosol science indicates that drops of respiratory fluid approximately 100 µm and less in diameter may float and evaporate faster than they fall to the ground (though it’s not a hard boundary),[6] and therefore for the purposes of this paper are termed aerosols (sometimes labelled droplet nuclei). For the purposes of this paper, respiratory fluid larger than 100 µm in diameter are labelled droplets and will generally fall to the ground faster than they evaporate.

Far-field aerosols refer to aerosols beyond six feet from an infected person, and their concentration level is generally closer to the whole room average aerosol concentration level than for near-field aerosols.[7] Near-field aerosols refer to aerosols within three to six feet of an infected person and occur at higher concentration levels than far-field aerosols (though as they dissipate throughout the room, they eventually become far-field aerosols). Far-field aerosols are impacted more than near-field aerosols by most of the mitigation strategies focused on by this model which also have very little to no impact on droplets (with settling and masks being the notable exception).

The objectives of this study are to (1) provide a detailed review on the mathematical models and the published data that describe droplet / aerosol generation and quantum generation of an infected occupant, removal and inactivation mechanisms and the corresponding infection risk reduction of different strategies; (2) develop a comprehensive model that can compare and rank those solutions; (3) validate the model against two documented super-spreading events of SARS-CoV-2 as well as (4) assess

the model's general effectiveness. The authors also discussed the model's limitations as well as its assumptions and justifications.

Modelling aerosol transmission and literature review

The probability of infection calculations used by the model of the Facility Infection Risk Estimator™[1] are based on a modified version of the Wells-Riley model of infection.[8,9] The starting point[9] for this model includes removal terms for ventilation, building system filtration, and settling. Removal terms for portable air cleaners, masks, inactivation from RH, and inactivation from upper room UVGI (ultraviolet germicidal irradiation) were subsequently added. The modified formula is Equation (1):

- $$P = \left[1 - \exp\left(\frac{-(q*I*p*s*t)}{V*\left(k_{settling} + \lambda_{ventilation} + k_{filtration} + k_{RHinactivation} + k_{GUVinactivation} + k_{aircleaner} + k_{mask}\right)}\right)\right] * v_{adjusted} \quad (1)$$

    - P = probability of infection
    - q = quantum of infection (quanta generation rate), discussed further below
    - I = number of infected individuals, discussed further below
    - p = pulmonary ventilation rate, discussed further below
    - s = modified p scaling factor for masks, discussed further below
    - t = time of exposure, discussed further below
    - V = volume of the room/space.
    - $k_{settling}$ = settling removal factor, discussed further below
    - $\lambda_{ventilation}$ = ventilation removal factor, discussed further below
    - $k_{filtration}$ = building system filtration removal factor, discussed further below
    - $k_{RHinactivationIVA}$ or $k_{RHinactivationSC2}$ = RH inactivation removal factor, discussed further below
    - $k_{UVGIinactivationIVA}$ or $k_{UVGIinactivationSC2}$ = upper room UVGI inactivation removal factor, discussed further below
    - $\lambda_{aircleaner}$ = portable air cleaner removal factor, discussed further below
    - k_{mask} = mask removal factor, discussed further below
    - $v_{adjusted}$ = adjusted vaccination factor, discussed further below

Quantum of infection

The Wells-Riley model is "… based on a concept of 'quantum of infection, whereby the rate of generation of infectious airborne particles (or *quanta* - *q*) can be used to model the likelihood of an individual in a steady-state well-mixed indoor environment being exposed to the infectious particles and subsequently succumbing to infection."[9]

The quanta generation rate, q, is a "hypothetical infectious dose unit" that is typically estimated using epidemiological studies. This single number, in units of 1/hr, is an amalgamation of "... the amount of particles generated over time and the infectivity of particles, which also inherently captures susceptibility of individuals and particle size effects such as the probability of deposition in relevant regions of the respiratory system" and must be determined for each pathogen.[8]

This model varies the quanta per hour by selected activity level and expiratory event, for either influenza or SARS-CoV-2. Both activity level, primarily through breathing (or pulmonary ventilation) rates, and expiratory means (speaking, breathing, coughing, etc.) influence the initial size and quantity of the virus-containing droplets / aerosols, the varying concentration levels of virus particles within the droplets / aerosols, the potential for a non-infected individual to breathe them in, and the potential that they will reach deep enough in the lungs to cause an infection. Therefore, they impact the quantum of infection value.

Table 1: Quantum generation rate estimate (quanta per hour)

Activity	Influenza Quantum Generation Rate Estimate (Quanta per hour)			SARS-CoV-2 Quantum Generation Rate Estimate (Quanta per hour)		
	Low Shedder	Medium Shedder	High Shedder	Low Shedder	Medium Shedder	High Shedder
Breathing / Resting	3.2	35.0	68.0	4.0	15.8	28.0
Speaking, Coughing, or Sneezing / Resting	6.6	72.3	140.5	16.0	50.2	85.7
Loudly Speaking or Singing / Resting	29.6	324.2	630.0	97.0	382.5	679.0
Breathing / Light	3.5	38.5	74.8	4.4	17.4	30.8
Speaking, Coughing, or Sneezing / Light	7.3	79.5	154.6	21.0	65.9	112.5
Loudly Speaking or Singing / Light	32.6	356.6	693.0	134.0	528.5	938.0
Breathing / Moderate	4.6	49.9	96.9	5.7	22.5	39.9
Speaking, Coughing, or Sneezing / Moderate	9.4	103.0	200.2	26.5	83.2	142.0
Loudly Speaking or Singing / Moderate	42.2	462.0	897.8	170.0	670.4	1190.0
Breathing / Heavy	10.6	116.3	226.1	13.3	52.5	93.1
Speaking, Coughing, or Sneezing / Heavy	22.0	240.4	467.2	63.7	199.9	341.3
Loudly Speaking or Singing / Heavy	98.6	1077.9	2094.8	408.0	1609.0	2856.0

Table 1 above lists the quantum generation rates by expiratory means / activity level for both influenza and SARS-CoV-2 that are used in this model. In addition, separate values are provided for low, medium, and high shedders. These values are taken directly from and/or estimated from the values and sources listed in Table 2 as well as the Airborne Infection Risk Calculator manual.[10] Due to conflicting data and opinions in the research relative to varying quantum generation rates between adults and children,[11,12] the model currently assumes the same rate for both children and adults.

The model allows the user to select from the following expiratory means: Breathing, Speaking, Loudly Speaking or Singing, Coughing, and Sneezing. These specific categories were used to coordinate the quanta generation by expiratory means with the droplet / aerosol size ranges produced by expiratory means (discussed below in the Settling Removal Factor section). The following activity levels are

available to select from: Resting (sitting, reading, sleeping, and watching TV), Light (standing and most domestic or office work), Moderate (climbing stairs and light exercise), and Heavy (vigorous exercise). These specific categories were used to coordinate the quanta generation by activity level with pulmonary ventilation rates, discussed further below.

Table 2: Referenced quantum generation rate studies

Activity	Virus	Quantum Generation Rate Estimate (Quanta per hour)	Notes
Breathing / Sitting	influenza	15 - 128[13]	Highly infectious / superspreader range
Breathing / Sitting	influenza	<3.2 - 20[14]	High degree of uncertainty
Breathing / Sitting	influenza	LR: 15; IR: 76.18; HR: 128[15]	LR, IR, HR - low, intermediate, high risk
Breathing / Sitting	influenza	515[16]	Airflight Outbreak / highly infectious
Breathing / Sitting	influenza	0.17 - 630[17]	LR/symptomatic to HR/asymptomatic
Breathing / Sitting	influenza	33.9 - 67.8[11]	No indication of level of risk / superspreader
Breathing / Sitting	influenza	68.67[18]	Mean value of Rudnick and Milton[13] - HR
Breathing / Sitting	SARS-CoV-2	<1[19]	Symptomatic infectious subject
Vocalization / Light Activity	SARS-CoV-2	>100 (1030)[19]	Asymptomatic infectious subject; walking slowly
Speaking / Light Activity	SARS-CoV-2	142[19]	Asymptomatic infectious subject; worst case
Breathing / Sitting	SARS-CoV-2	LR: 11.4; IR: 28.94; HR: 295.5[15]	Using SARS-CoV-1 as a proxy
Breathing / Sitting	SARS-CoV-2	0.36[20]	Asymptomatic subject; Assuming low risk; Preprint
Breathing / Heavy Activity	SARS-CoV-2	2.4[20]	Asymptomatic subject; Assuming low risk; Preprint
Speaking / Light Activity	SARS-CoV-2	4.9[20]	Asymptomatic subject; Assuming low risk; Preprint
Singing / Light Activity	SARS-CoV-2	31[20]	Asymptomatic subject; Assuming low risk; Preprint
Singing / Light Activity	SARS-CoV-2	970 [680-1190][21]	Asymptomatic; High Risk (superspreader); Preprint
? (Breathing / Sitting)	SARS-CoV-2	14 - 48[22]	Fitted quantum generation rate w/ R0; Preprint

Oral Breathing (Lecturing)	SARS-CoV-2	4.4[12]	Assuming low risk
Speaking (Lecturing)	SARS-CoV-2	21[12]	Assuming low risk
Loud Speaking (Lecturing) / Singing	SARS-CoV-2	134[12]	Assuming low risk
Oral Breathing / Sitting (Student)	SARS-CoV-2	4[12]	Assuming low risk
Speaking / Sitting (Student)	SARS-CoV-2	16[12]	Assuming low risk
Loud Speaking (sitting) / singing	SARS-CoV-2	97[12]	Assuming low risk

Number of infected individuals

The model allows the option of selecting one or more infected individuals. Each infected individual is assumed to have the same expiratory means, activity level, quantum of infection, and pulmonary ventilation rate.

Pulmonary ventilation (breathing)

Breathing rate is important to consider as it impacts the amount of virus potentially inhaled. It is also important to factor in the variation between adults and children. Adult and child pulmonary ventilation rates by activity level are determined using Table 6-31 from the EPA's Exposure Factors Handbook.[23] The Total Daily IR (inhalation rate) value for an adult average, divided by 24 hours, was used to provide the adult pulmonary ventilation rate for these calculations, representing ages 18 and older. The Total Daily IR value for a 10-year-old child, divided by 24 hours, was used to provide the child pulmonary ventilation rate for these calculations, representing ages less than 18 years of age.

Modified p scaling factor (masks)

The mask effective efficiency value, discussed further below in the Removal and Inactivation Factors section, is used to calculate a scaling factor that scales the rate at which quanta of infection are breathed in as a result of wearing a mask.[24] This is described by Equation (2)

- $$\text{modified p scaling factor(s)} = 1 - (\text{mask effective efficiency} * \%\ \text{non} - \text{infected wearing a mask}) \quad (2)$$

The unmodified p scaling factor (1 – mask effective efficiency)[24] was modified to account for the potential that not all non-infected individuals are wearing a mask. The model allows one to input the percentage of infected and non-infected individuals wearing a mask. The unmodified p scaling factor values used for the different mask types are listed below in Table 5, discussed in the Removal and Inactivation Factors section.

Time of exposure

The model allows one to enter the time of exposure in hours. Exposure time will vary by a) facility type, b) the different occupants present in the facility, and c) the different activities they undertake during the day. For example, if an infected individual is present in a room, the exposure time of elementary students could be significantly more than an office worker meeting with an infected coworker for 20 minutes in a conference room.

Removal and inactivation factors

Research indicates aerosol transmission is likely a predominant route for the transmission of many viruses,[8,25,26] including influenza and SARS-CoV-2. Reducing the threat from virus-containing aerosols indoors, once the virus particles have been expirated from an infected person, is accomplished by removing or inactivating them before non-infected individuals have an opportunity to inhale them. The removal and inactivation mechanisms addressed in this model include settling (via gravity), ventilation (via outdoor air), filtration (via the building HVAC system, portable air cleaners, and/or mask wearing), and virus inactivation (via relative humidity and/or upper room UVGI). Each of these is discussed in more detail below.

Settling removal factor

Environmental conditions impact the rate of settlement due to gravity. Air flow may keep smaller droplets / aerosols in the air longer and relative humidity (RH) plays a large role in the size of the droplets / aerosols after leaving the infected host.[26,27] Droplets evaporate faster at lower RH levels, increasing their likelihood of staying aloft longer. Temperature also affects settling velocity through its impact on the dynamic viscosity of air; the warmer the temperature the higher the dynamic viscosity and the slower the settling velocity. As the dynamic viscosity of air doesn't vary significantly over the narrow temperature setpoint range found in most occupied spaces (68^{O}F - 76^{O}F (20^{O}C - 24.4^{O}C)),[28] the dynamic viscosity for a temperature of 72.5^{O}F (22.5^{O}C) at one atmosphere of pressure is used for this model.

The means of expiration must also be considered because they impact the quantity and size of virus-containing droplets / aerosols that are released from an infected individual. This model uses a weighted average initial diameter for these droplets / aerosols (immediately after expiration) to estimate the removal efficiency associated with settling and the associated impact on the probability of infection. Table 3 provides the average initial droplet / aerosol diameters used by this model for the following expiratory means: breathing, speaking normally, speaking loudly, singing, coughing, and sneezing, based on the references listed.

Table 3: Initial and equilibrium droplet / aerosol weighted average GM by expiratory means

Measurement Range (μm)	Expiratory Event	Droplet GM (μm) Calculated by the team	% Infectious Droplets or % Concentration	Calced Droplet GM (μm)	% Infectious Droplets or % Concentration	Calced Droplet GM (μm)	% Infectious Droplets or % Concentration	Calced Droplet GM (μm)	% Infectious Droplets or % Concentration	Calced Droplet GM (μm)	% Infectious Droplets or % Concentration	Weighted Average GM (μm)	Equilibrium vs Initial	Estimated Initial Weighted Average GM (μm)
0.3-?	Breathing	0.4	70%	0.7	17%	2.2	13%					0.7	Assumed Equil.	1.4[14]
0.3-10	Breathing	0.4	82%	2.2	18%							0.7	Assumed Equil.	1.4[29]
0.05-50	Breathing	0.2	90%	5.0	10%							0.7	Assumed Equil.	1.3[30]
0.5-20	Breathing	0.8	86%	1.8	9%	3.5	3%	5.5	2%			1.1	Assumed Equil.	2.1[31]
0.3-20	Breathing	0.6	64%	1.1	36%							0.7	Assumed Equil.	1.5[32]
											~~Breathing Average~~	~~0.8~~		~~1.5~~
											Breathing Average, Infected Only	0.7		1.4
0.5-20	Speaking softly	0.8	85%	1.8	11%	3.5	3%	5.5	1%			1.0	Assumed Equil.	2.1[31]
0.5-20	Speaking normal	0.8	73%	1.8	21%	3.5	2%	5.5	4%			1.3	Assumed Equil.	2.5[31]
0.3-20	Speaking normal	0.5	79%	1.3	21%							0.7	Assumed Equil.	1.3[32]
0.3-20+	Speaking normal	0.8	43%	1.2	54%	145	3%					5.3	Equil.	10.7[33]
0.3-20+	Speaking normal	0.8	44%	1.2	56%							1.0	Equil.	2.1[33]
0.5-20	Speaking loudly	0.8	69%	1.8	13%	3.5	13%	5.5	5%			1.5	Assumed Equil.	3.0[31]
0.3-20	Speaking loudly	0.5	39%	1.3	61%							1.0	Assumed Equil.	2.0[32]
											~~Speaking Normal Average w/ O-mode~~	~~2.4~~		~~4.8~~
											Speaking Normal Average w/out O-mode	1.0		2.0
											Speaking Loudly Average	1.3		2.5

0.3-20	Singing average	0.5	44%	1.1	56%							0.9	Assumed Equil.	1.7[32]
0.3-20	Singing loudly	0.6	34%	1.3	66%							1.0	Assumed Equil.	2.1[32]
Singing Average												1.0		2.1
?	Cough	0.5	15%	1.7	25%	5.5	60%					3.8	Assumed Equil.	7.6[9]
?	Cough	0.5	35%	2.0	23%	6.3	42%					3.3	Assumed Equil.	6.6[34]
0.3-?	Cough	1.5	100%									1.5	Assumed Equil.	3.1[35]
0.5-20	Cough	0.8	83%	1.8	14%	3.5	2%	5.5	1%			1.0	Assumed Equil.	2.1[31]
0.3-20+	Cough	0.8	40%	0.8	54%	123.0	6%					8.1	Equil.	16.3[33]
0.3-20+	Cough	0.8	43%	0.8	57%							0.8	Equil.	1.6[33]
~~Coughing Average w/ O-mode~~												~~3.6~~		~~7.1~~
~~Coughing Average w/out O-mode~~												~~2.1~~		~~4.2~~
Coughing Average, Infected Only												2.9		5.8
0.1-1000	Sneeze	Unimodal distribution; size class w/ most droplets: 341.5 - 398.1 µm										360.1	Assumed Initial	NA[36]
0.1-1000	Sneeze	Bimodal distribution; size class w/ most droplets: 73.6 - 85.8 µm										74.4	Assumed Initial	NA[36]
?	Sneeze	1.4	3%	2.8	16%	5.7	35%	11.3	28%	126.5	19%	29.0	Assumed Initial	NA[37]
	~~Sneezing Average~~											~~154.5~~		~~NA~~
	Sneezing Average, Excluding Unimodal distribution											51.7		NA

The table lists different measured droplet / aerosol (particle) diameter ranges (first column) associated with a specific expiratory means (second column) pulled from the various studies referenced in the last column. Within that overall range, as provided by the studies, the subsequent series of paired columns list a) calculated GMs (geometric mean diameters) for various bins of particle size ranges and b) an associated percentage. This percentage consists of either a) the percentage of infectious particles within the bin relative to the infectious particles from the overall particle size range or b) the percentage concentration of particles within the bin relative to the concentration of particles from the overall particle size range. For the referenced studies where it was possible, these series of paired columns are used to calculate the weighted average GM (third column from the end) using the following method[9]. The percentages of infectious particles contained within each associated bin of droplet / aerosol (particle) distribution ranges were multiplied by the GM from each of these bins, and then these products added together to get the weighted average GM for each referenced study.

However, because only a few studies involved infected volunteers, additional studies involving healthy individuals also had to be referenced. In these cases, the percentage concentration for each bin of droplet / aerosol size ranges as opposed to the percentage of infectious particles contained within each bin was used to determine the weighted average GM. Most of the studies reported equilibrium sizes for the droplet / aerosol size ranges (or were assumed to), which are the size of droplets / aerosols after reaching equilibrium with environmental conditions, primarily driven by RH.[38] To estimate the initial weighted average GM (the last column), the equilibrium sizes were divided by an evaporation factor of 0.5.[33]

For each expiratory means, the size values from the relevant studies were averaged together to reach the final weighted average values used by the model. Where possible, the final selected average was determined from studies making use of only infected individuals. O-mode size distribution ranges were excluded due to available research suggesting greater concentrations of viral particles occur in smaller droplets / aerosols.[14,27,30,31,34,35,39,40,41] These and other averages discarded for use in the model are crossed out in the table. In order to coordinate with the quanta generation by expiratory means (discussed above), speaking loudly and singing were combined into a single expiratory event, using the initial droplet / aerosol diameters for speaking loudly.

To calculate the settling removal efficiency ($E_{settling}$), the initial and equilibrium droplet / aerosol diameters are needed. As discussed above, Table 3 provides the average initial droplet / aerosol diameters used by this model. Equilibrium particle diameters are then calculated using an average of the model-based experimentally derived respiratory droplet size transformation ratios (the last column in Table 4) that corresponds to the relevant room RH, shown in Table 4.[38]

Table 4: Respiratory droplet / aerosol size transformation average D_{eq}/D_i ratios

RH	Model-based D_{eq}/D_i ratios			Experimentally derived D_{eq}/D_i ratios	Average D_{eq}/D_i ratios
	D_i = 0.1 µm	D_i = 1.0 µm	D_i = 10.0 µm		
10%	0.401	0.402	0.402	0.391	0.399
20%	0.407	0.407	0.407	0.395	0.404
30%	0.412	0.412	0.412	0.398	0.409

40%	0.416	0.417	0.417	0.401	0.413
50%	0.422	0.423	0.424	0.427	0.424
60%	0.429	0.431	0.432	0.437	0.432
70%	0.439	0.443	0.444	0.449	0.444
80%	0.456	0.464	0.465	0.464	0.462
90%	0.49	0.513	0.516	0.502	0.505

Settling velocities are calculated referencing particle densities[42] and the Stokes Law formula;[38] $v = (g * D_{eq} * \rho) / (18 * \mu)$; g = gravitational acceleration, ρ = particle density, μ = dynamic viscosity of air. The final formula for $k_{settling}$ is Equation (3).

- $k\text{settling} = v/H$ (3)
    - v = settling velocity
    - H = height of the room/space

Ventilation removal factor

Ventilation refers to the introduction of outside air into a space. It has the impact of diluting contaminants, including virus-containing aerosols, which in turn increases the amount of time required to inhale an infectious dose of virus. The continued introduction of outside air also displaces the same amount of air within the space, removing contaminants in the process, though due to mixing it is not an immediate one to one replacement.[8,27,43]

Ventilation may be supplied mechanically through HVAC systems or naturally through operable windows or other intentional or unintentional openings in the building envelope. Recommended ventilation rates will vary depending on factors such as the space or facility type, the activities being conducted, and the density of people present. Ventilation removal efficiency ($E_{ventilation}$) is dependent on ventilation rates for the room/space in question and entered as the total OA (outside air) in cubic feet per minute (cfm). $k_{ventilation}$ equates to the outside air changes per hour for the room/space, calculated using the entered OA per space and the space volume. Design ventilation rates are often not readily available unless one has access to as-built drawings and actual ventilation rates will often vary from design ventilation rates. Engineers, commissioning agents, and/or test and balance (TAB) consultants may need to be consulted to verify actual ventilation rates or determine a close approximation.

Filtration removal factor – filters inside building systems

Filtration refers to a physical medium used to "capture" contaminants, including droplets / aerosols, from the air as it passes through the medium. For building systems, filters follow a Minimum Efficiency Reporting Values (MERV) rating system, with values ranging from 1 on the low end all the way up to 16. The ratings provide an indication of how effective a filter is at removing particles of varying size ranges out of the air.[8,9,44] Filtration is effective if a) the contaminants are airborne, such as virus-containing aerosols, and b) the clean air delivery is high enough.[8,9,45,46,47] Clean air delivery is a function of the filter's efficiency and the recirculated air rate.

The building system filter removal efficiency (η_{filter}) percentages for various MERV and HEPA ratings used are taken from aerosol-weighted values given in another source's Table 4.[9] The available MERV and HEPA input selections are limited to the levels used in this table. Users must select the value closest to

their existing and/or proposed conditions. Recirculated air changes per hour ($\lambda_{recirculation}$), entered as CFM per space, are needed to calculate the overall filtration removal efficiency ($E_{filtration}$). The final formula for $k_{filtration}$ is Equation (4).

- $\mathrm{kfiltration} = \lambda\mathrm{recirculation} * \eta\mathrm{filter}$ (4)
    - $\lambda_{recirculation}$ = recirculated air changes per hour for the room/space
    - η_{filter} = building system filter removal efficiency

As with ventilation rates, engineers, commissioning agents, and/or TAB consultants may need to be consulted to determine what filter rating and recirculated air rate should be used.

Filtration removal factor - portable air cleaners

Portable air cleaners are also available for use to supplement building system filtration and ventilation. Units sold in the U.S. should have a clean air delivery rate (CADR) corresponding to a recommended room volume. This model requires entering the CADR value of the unit(s) being used, and these ratings are typically provided by the manufacturer for smoke, dust, and pollen. Some research[14,34,48,49 ,50] suggests that a greater percentage of infectious viral particles (approximate 60% to over 90% for the studies referenced) are found in smaller droplets / aerosols, potentially 5 microns or less in diameter. This droplet / aerosol size range is more reflective of smoke and dust than pollen,[51] therefore this model requires the average of the smoke and dust CADR rating be entered.

The removal rate per portable air cleaner, $\lambda_{aircleaner}$, equals the CADR (clean air delivery rate) value from the manufacturer divided by the space volume (V),[51] as shown in Equation (5).

- $\lambda\mathrm{aircleaner} = \mathrm{CADR} / \mathrm{V}$ (5)

This value is then multiplied by the number of portable air cleaners being used per space to provide the total removal rate (1/h).

Filtration removal factor - masks

The last type of filtration accounted for by this model are masks, which block large droplets and filter a percentage of virus-containing aerosols from the air exhaled by an infected individual as well as from the surrounding air before they are inhaled by a non-infected individual.[30,52] The efficiency of a mask, or the percentage of aerosols with virus particles filtered out, depends on a) the removal efficiency of the mask material itself relative to the different size distributions of droplets / aerosols and flow rate through the mask and b) the leakage that occurs around the mask edges.[24,53,54,55,56,57,58,59]

Leakage is largely related to how well the mask fits a person. The pressure drop across the mask material also impacts its usability as the greater the pressure drop, the harder it is to breathe through. Greater pressure drops may also result in greater leakage rates, especially if the fit is poor because more particles will follow the path of least resistance through the gaps between the face and mask. The mask removal efficiency (E_{mask}) is calculated looking at the following two components, added together.

Mask removal efficiency, part 1: This part consists of the amount of droplets / aerosols removed from the room air by the masks of the non-infected individuals as they breath in (Equation (6) below) and is a small contribution compared to part 2. It is calculated using the mask effective efficiency (η_{mask}), the

number of non-infected individuals wearing them, and the estimated breathing generated air change rate across an individual mask of 1.2 cfm (2.0 m^3/hr),[56] as shown in Equation (6)

$$\text{mask removal for non} - \text{infected} = \left(\frac{1.2\text{cfm} * \%\ \text{non-infected wearing mask} * \text{number of non-infected occupants} * \frac{60\text{minutes}}{\text{hr}}}{\text{room volume}}\right) * \text{mask effective efficiency} \quad (6)$$

The estimated breathing generated air change rate used here represents respiration rates at rest. This model uses Mask Effective Efficiency (η_{mask}) values shown in Table 5 below (labelled Fitted Filtration Efficiency (%)). These come from a study[54] that directly measured the fitted filtration efficiency (FEE), accounting for both mask efficiency and face seal leakage, or mask fit.

In this study the FixTheMask add on consisted of a rubber band configuration mimicking the impacts of the FixTheMask mask fitter, resulting in a measured FFE of 78.2%. Another study[60] actually tested the manufactured FixTheMask mask fitter on a procedure mask using a similar particle range as the above study, though manikins were used instead of an actual person. The effective mask efficiency, or fitted filtration efficiency, was found to be 94.9%. For the model, these two values were averaged, giving an FFE of 86.6%.

Table 5: Filtration efficiencies and p scaling factor for masks used in this model[54]

	Fitted Filtration Efficiency (%) 0.2 µm - 0.3 µm	p scaling factor
No mask	0	0
2-layer woven nylon mask w/ ear loops w/out aluminium nose bridge	44.7%	55.3%
2-layer woven nylon mask w/ ear loops, w/ aluminium nose bridge	56.3%	43.7%
2-layer woven nylon mask w/ ear loops, w/ aluminium nose bridge & 1 nonwoven insert	74.4%	25.6%
Cotton bandana, folded "bandit" style	49.0%	51.0%
Single-layer woven polyester gaiter/neck cover	37.8%	62.2%
Single-layer woven polyester/nylon mask w/ ties	39.3%	60.7%
Nonwoven polypropylene mask w/ fixed ear loops	28.6%	71.4%
3-layer woven cotton mask w/ ear loops	26.5%	73.5%
Surgical mask w/ ties	71.5%	28.5%
Procedure mask w/ ear loops	38.5%	61.5%
Procedure mask w/ ear loops & 3D printed ear guard	61.7%	38.3%
Procedure mask w/ ear loops & FixTheMask	86.6%	13.4%
N95	98.4%	1.6%

Mask removal efficiency, part 2: This part consists of the amount of droplets / aerosols removed by the masks from the air breathed out by the infected individual(s), before they enter the room air, as shown in Equation (7).

- $\text{source reduction} = (\text{mask effective efficiency} * \%\ \text{infected wearing a mask})$ (7)

The final formula for k_{mask} is then Equation (8).

- $\text{kmask} = (\text{mask removal for non} - \text{infected} + \text{source reduction})$ (8)

Inactivation – RH removal factor

Inactivation refers to a process of rendering a virus non-infectious. This model focuses on two types of inactivation. The first is in relation to relative humidity (RH), as research indicates that for typical interior temperature ranges, most viruses, including membrane-bound viruses like SARS-CoV-2 and influenza, find low (< 40%) and high (>90%) RH levels more conducive to survival with increased decay rates occurring at intermediate RH levels.[25,27,61,62,63] As droplets / aerosols evaporate after expiration, the concentration levels of proteins, salts, etc., within them increase, creating conditions unfavourable to the virus and likely speeding up its inactivation, though additional research is needed to understand the nuances of how this varies by virus type, strain, phenotypic characteristics, temperature, and specific respiratory fluid characteristics. For the purposes of this model, a linear relationship is assumed for influenza[27] and SARS-CoV-2.[64]

While temperature impacts virus inactivation,[25] there doesn't does not appear to be significant variation in virus decay over the narrow temperature setpoint range found in most occupied spaces, 68^{O}F - 76^{O}F (20^{O}C - 24.4^{O}C).[27] For the purposes of the model, an interior temperature of 22.5°C (72.5°F) and associated dynamic viscosity of air of 1.83x10^{-5} is assumed. For SARS-CoV-2, an interior temperature of 72^{O}F (22.2 ^{O}C) is assumed to coordinate the constraints of the Department of Homeland Security calculator[64] used to estimate the virus' inactivation due to RH (discussed further below). These assumptions also coordinate with the interior temperature assumptions made for settling discussed above.

The influenza A virus inactivation rate ($k_{RHinactivationIVA}$) due to relative humidity (RH) entered is calculated using Equation (9)[38]

- $\text{kRHinactivationIVA} = (0.0438 * \text{RH}) - 0.00629$ (9)

For SARS-CoV-2, the inactivation rate ($k_{RHinactivationSC2}$) is calculated using Equation (10)

- $\text{kRHinactivationSC2} = (0.0135 * \text{RH}) - 0.0028$ (10)

The equation was developed using a web application developed by the Department of Homeland Security.[64] Decay rates were determined using this calculator for a UV Index of 0 (inside) and an interior assumed temperature of 72^{O}F (22.2^{O}C) to correspond to assumptions made for influenza and droplet evaporation. Note that the Department of Homeland Security calculator only provided values between a RH of 20+% and 70%. Table 6 then converts these values to 1/min, which were then graphed and Equation (10) formulated for the 99% decay rate values.

Table 6: SARS-CoV-2 inactivation / decay rate (min^{-1})

RH	50% Decay (min^{-1})	90% Decay (min^{-1})	99% Decay (min^{-1})
21%	0.000406702	0.000122441	6.12205x10^{-5}
22%	0.001304121	0.000392711	0.000196356
23%	0.002201673	0.000662954	0.000331477
25%	0.003996803	0.001203369	0.000601685

30%	0.008503401	0.002556237	0.001277139
35%	0.013020833	0.003903201	0.001953888
40%	0.01754386	0.005257624	0.002628812
45%	0.021929825	0.006613757	0.003306878
50%	0.026455026	0.007974482	0.003977725
55%	0.030864198	0.009310987	0.004655493
60%	0.035460993	0.010683761	0.005324814
65%	0.03968254	0.011990408	0.006016847
70%	0.043859649	0.013333333	0.00669344

Inactivation – upper room UVGI removal factor

The second type of inactivation focused on in this model is Upper Room UVGI (ultraviolet germicidal irradiation). A sufficient dosage of ultraviolet radiation will inactivate viruses (by photochemical disruption of viral RNA upon absorbing UV photons), with the UV-C band of energy (wavelengths between 100 and 280 nm) having the greatest germicidal effect.[43,65,66,67] Upper room applications of this technology make use of UV radiation generating lamp sources (low/medium pressure mercury vapor lamps or UVC-LEDs), either wall mounted or suspended from the ceiling, to irradiate upper air zones of individual spaces while shielding the lower occupied zones from harmful UV radiation.[66,67,68,69,70,71] Substantial evidence exists for the effectiveness of Upper Room UVGI systems in killing various pathogens, including coronaviruses.[46,72]

Germicidal effectiveness of these systems is influenced by spatial configuration, the location, number, and power of the UV fixtures, relative humidity, the airflow and air mixing that occurs between the lower occupied zone and upper irradiated zone, and the type of pathogen and its source(s). Of all these influences, the air up flow rate perhaps has the most impact, as this determines the speed with which pathogens are carried up into the irradiated zone to be eliminated, as well as how long they are irradiated, impacting the dose received. However, this simplified model assumes a well-mixed condition and only indirectly accounts for the impact of the airflow rate and ACH (discussed further below).

The upper room UVGI coefficient of inactivation (or removal factor) is calculated by multiplying the UVGI system's upper room average irradiance or fluency (E) by the relevant susceptibility parameter (Z) for either influenza or SARS-CoV-2,[66,67,68,69,70,73,74,75,76,77] as shown in Equation (11)

- $[\mathrm{kUVGIinactivationIVA\ or\ kUVGIinactivationSC2}] = \mathrm{E} * \mathrm{Z}$ (11)

Sources, including the 2009 NIOSH application guideline, recommend that the upper room average irradiance (E) should generally fall within the range of 30 - 50 µW/cm^2 for most pathogens.[67,75]

But the final average value depends on the number of lamps, their individual output, fixture configuration, fixture layout, and room parameters. Measured and modelled values often fall below this range.[67,70,75] It will likely be necessary to coordinate with a design engineer and/or manufacturer to determine an appropriate estimate for a given setting. For these calculations, the effective average irradiance (E) for the whole space is used instead of the upper room average irradiance and is estimated by multiplying the upper room average irradiance by the ratio of upper room volume to total room volume.[75,78] Under well mixed conditions (obtained via ceiling fans, the building mechanical system, or

some combination), some research[78] indicates the whole room average irradiance value adequately accounts for the effects of air turnover rates between the upper and lower zones for all fan speeds of conventional low-velocity ceiling fans. Though potential conditions of stagnation or greater than six ACH[43] will likely produce results overestimating the effectiveness of the upper room UVGI system.

Reported susceptibility parameter (Z), or UV rate constant, values (m^2/J) for influenza A include 0.15,[73] 0.27,[79] 0.29 at 25-27% RH,[74] 0.27 at 50-54% RH,[74] and 0.22 at 81-84% RH.[74] In order to tie the Z value to RH, the last three values were used; see Table 7 below. The second RH range column was added to tie it to the RH ranges accounted for by this model.

Table 7: Estimated Z values for influenza aerosols determined at low, medium, and high relative humidity (modified from table 1[74])

RH range (%)	RH Range (%)	Estimated Z Value (m^2/J)	95% Confidence Interval		R^2
			Lower	Upper	
25 - 27	0% - 33%	0.29	0.27	0.31	0.985
50 - 54	34% - 66%	0.27	0.26	0.31	0.991
81 - 84	67% - 100%	0.22	0.21	0.23	0.992

Reported susceptibility parameter (Z), or UV rate constant, values (m^2/J) for SARS-CoV-2 include the suggestion[16] for 0.377 (best-case) and 0.0377 m^2/J (worst-case) and the suggestion[72] of 0.05524 m^2/J. At this point there are no known studies linking the susceptibility parameter (Z) for SARS-CoV-2 to RH, so for the purposes of this model, an average of 0.377 and 0.0377 m^2/J was used (0.207 m^2/J).

The relationship between ACH, ventilation and UVGI is not fully understood.[24] Greater ACH levels within lower ranges can positively impact room mixing, aiding in UVGI's effectiveness by increasing the percentage of pathogens exposed at a faster rate. But greater ACH rates also decrease its effectiveness relative to delivered dosage by decreasing the amount of exposure time for the pathogens in question. Future versions may look at incorporating these parameters, but for now the effective average irradiance for the whole space is used to partially account for not directly estimating the impacts of ACH or air turnover rates on delivered dosage, as discussed above.

Adjusted vaccination factor

The model also accounts for the impacts of vaccination for influenza. Default influenza U.S. coverage rates for children (57%) and adults (42%) are provided based on averages of nine consecutive flu seasons for each, calculated from data provided by the CDC.[80] However, users of the model may modify these default values if desired. As COVID vaccinations are still rolling out and yet to be approved for children under 12 (as of this paper's publication), local vaccination percentages are recommended to be used to guide the input for the percentage of adults and children 12 and over who are vaccinated.

To integrate the impact of vaccination into these calculations, the relationship between the probability of infection calculated by this model and the basic reproduction number, R_0 is used. R_0 is "... defined as the expected number of secondary cases produced by a single (typical) infection in a completely susceptible population,"[81] and the probability of infection is one of three factors multiplied by each other to calculate R_0.

The impact of vaccination on the reproduction number can be estimated using Equation (12).

- $\mathrm{R0p} = (1 - \mathrm{p}) * \mathrm{R0}$ (12)

"where R_{0p} is the R_0 under vaccination and p is the vaccination coverage rate of the population who have been vaccinated."[11] This model uses the relationship between R_0 and the probability of infection to estimate the impact of vaccination on the probability of infection, essentially multiplying it by (1-p). As vaccinations are not 100% effective, the p value for children and adults is also multiplied by estimates of influenza vaccination effectiveness for children (0.70) and adults (0.62).[82] This provides the adjusted vaccination factor ($v_{adjusted}$) applicable for influenza.

For SARS-CoV-2, adult efficacy percentages for the most prominent vaccines are listed in Table 8 (also used as a proxy for those 12 to 15 years of age as of this paper's publication. These have been obtained from the sources listed for each vaccine. As indicated in the table, the efficacies for Johnson and Johnson were determined for both moderate to severe and severe symptoms. Cells with dashes indicate no formal efficacy values are available at this point. Though preliminary data does indicate the efficacy of the Pfizer and Moderna vaccines is less for the variants. Due to limited data and uncertainty regarding the variants, it was decided to use one estimated efficacy value, averaging all of the percentages listed in Table 8 together, resulting in a value of 0.80. As more efficacy data becomes available, the model will be updated. The model currently does not allow one to account for any immunity generated through previous community infections. In those cases where a large number of such individuals (who are also unvaccinated) may be present within a building population, the results will overestimate the probability of infection to an unknown degree.

Table 8: SARS-CoV-2 Vaccine Efficacy

Vaccine	Adults							
	Original		B.1.1.7 (UK)		B.1.351 (South African)		P.1 (Brazil)	
	Symptomatic - moderate to severe	Symptomatic - severe	Symptomatic - moderate to severe	Symptomatic - severe	Symptomatic - moderate to severe	Symptomatic - severe	Symptomatic - moderate to severe	Symptomatic - severe
Pfizer–BioNTech[83,84]	94.8%		--	--	--	--	--	--
Moderna[83,84]	94.1%		--	--	--	--	--	--
Johnson and Johnson[83,85]	72.0%	85.0%	--	85.0%	57.0%	85.0%	66.0%	85.0%
Novovax[86]	95.6%		85.6%		60.0%		--	--
Overall Average	**80.4%**							

Validation of model against previous infection cases

To demonstrate the strengths and weaknesses of the web application[1] and its underlying model, it has been used to model the outcomes of two documented superspreading events: the Skagit Valley Chorale Superspreading Event[21] and the Guangzhou Restaurant Event.[87,88,89]

Skagit Valley chorale superspreading event

In March of 2021, a COVID-19 outbreak occurred as the result of a choral practice at the Mount Vernon Presbyterian Church in Skagit Valley, Washington, U.S. One symptomatic individual attended the choral practice which included a total of 61 vocalists. After the practice, 53 members were confirmed through testing or were strongly suspected of as having contracted COVID-19 from reported symptoms. A detailed analysis of this likely superspreading event was previously performed,[21] assuming transmission was predominantly via virus-containing aerosols and using gathered data to infer the quanta generation rate of aerosols emitted by the infected individual. Based on this previous analysis and data gathered to perform it the following parameters were entered into the model.

Rehearsal hall room size: 1,937.5 ft^2 (180 m^2), 14.76 ft (4.5 m) ceiling.[21]

Design OA: 1,236 cfm (2,100 m^3/hr). The referenced analysis[21] used ASHRAE Standard 62.1 and existing mechanical drawings to estimate the design ventilation, or outside air (OA), for the rehearsal hall.

Design RA: 3,473 cfm (5,900 m^3/hr). The referenced analysis[21] used ASHRAE Standard 62.1 and existing mechanical drawings to estimate the design recirculated air (RA) for the rehearsal hall.

Choir practice OA: 334 cfm (567 m^3/hr), +/- 50% uncertainty: 167 cfm (284 m^3/hr) – 501 cfm (850 m^3/hr). Based on the data gathered, the referenced analysis[21] assumed the HVAC fan wasn't operating during the choir practice, providing no mechanical outside or recirculated air (the body heat from the number of choir members present was sufficient to maintain a comfortable temperature). Based on the delta between exterior and interior temperatures during the practice, the estimated body heat generated by individual choir members, and the heat capacity of air, an estimate was made by the referenced analysis[21] of the amount of outside air that entered via infiltration, along with values representative of +/- 50% uncertainty.

Choir practice RA: 0 cfm (0 m^3/hr).[21] The system was not running at the time of the event.

Furnace filter: MERV 11.[21]

Temperature: Thermostat setting: 68 ^{O}F (20 ^{O}C), assumed interior temperature: 71 ^{O}F (22 ^{O}C), determined from gathered data.[21] The interior temperature fits within the 68^{O}F - 76^{O}F (20^{O}C - 24.4^{O}C) that this model is currently optimized for.

Relative humidity (RH): 30% RH. No RH information for the rehearsal hall room during the practice was provided.[21] Nor was the use of any type of humidifier indicated. As the heater had been on to warm the space before choir members arrived, the air was assumed to be at a lower humidity than if the heater had not been running. Deviations from this estimation are discussed below.

Number of infected individuals: 1. The referenced analysis[21] made this estimation based on one choir member having "cold-like" symptoms manifesting three days prior to the practice and subsequently testing positive for COVID-19.

Viral shedding level: High. Referencing other published analyses of COVID-19's incubation time, the referenced analysis[21] estimates that such a high secondary attack rate resulting from one infected person would require high shedding of the virus by the infected individual.

Activity level: Light. Choral members were generally sitting while practicing with some limited standing and walking.[21] Holding music and singing while sitting would be more along the lines of office work as opposed to passively sitting while resting. Therefore a "light" activity level was selected, which would also encompass standing and leisurely walking for short distances.

Number of choral members present: 61.[21] This includes the infected individual.

Expiratory Means / Exposure Time: The following breakdown was selected for this analysis. The probability of infection was calculated for each time period and the net probability of infection determined from these three individual values.

- Singing / 126 minutes (2.1 hours)
- Speaking / 18 minutes (0.3 hours)
- Breathing Only / 6 minutes (0.1 hours)

The total rehearsal time was determined to be 2.5 hours,[21] broken up as follows:

- Phase 1: 45 minutes with the 61 choral members all together in the Fellowship Hall. This time was spent primarily practicing with a brief amount of time transitioning to the next phase.
- Phase 2: 45 minutes spent primarily practicing in two groups. Group 1 consisted of approximately 35 people practicing in the Fellowship Hall and group 2 consisted of approximately 26 people practicing in the sanctuary. The infected person was part of Group 1.
- Break: 10 minutes with everyone talking and eating snacks.
- Phase 3: 50 minutes with the 61 choral members practicing all together in the Fellowship Hall.

To simplify the analysis, Phase 2 was modelled as the same conditions in Phase 1. This was decided due to a) lacking dimensional and ventilation information for the sanctuary and b) the infected person being part of the group practicing in the Fellowship Hall. In addition, an average amount of time of singing vs speaking vs breathing over the 2.5 hours was estimated referencing the answers provided by the choir spokesperson.[21]

Table 9 provides a) the resulting probability of infections calculated using this model, given the above estimations and b) the potential resulting number of additional people infected given the net probability of infection. The probability of infection for the three different expiratory means / exposure times are listed as well as the resulting net probability (the chance that at least one of these three conditions occurs). The net probability is calculated as shown in Equation (13).

- $$\mathrm{NPI} = (\mathrm{PIsinging} + \mathrm{PIspeaking} + \mathrm{PIbreathing}) - (\mathrm{PIsinging} * \mathrm{PIspeaking}) - (\mathrm{PIsinging} * \mathrm{PIbreathing}) - (\mathrm{PIspeaking} * \mathrm{PIbreathing}) + (\mathrm{PIsinging} * \mathrm{PIspeaking} * \mathrm{PIbreathing}) \quad (13)$$
    - NPI = Net Probability of Infection
    - $\mathrm{PI}_{\mathrm{singing}}$ = Probability of Infection - Singing
    - $\mathrm{PI}_{\mathrm{speaking}}$ = Probability of Infection - Speaking
    - $\mathrm{PI}_{\mathrm{breathing}}$ = Probability of Infection - Breathing

The number of additional people infected is 60 uninfected individuals multiplied by the net probability of infection.

Table 9: Probability of infections and resulting additional choral members potentially infected.

	Choral Practice Conditions			Design OA & RA
	OA - 167 cfm (284 m^3/hr)	OA - 334 cfm (567 m^3/hr)	OA - 501 cfm (850 m^3/hr)	OA - 1236 cfm (2,100 m^3/hr); RA - 3,473 cfm (5,900 m^3/hr)
Probability of Infection - Singing	96.0%	83.8%	71.8%	16.8%
Probability of Infection - Speaking	5.5%	3.1%	2.2%	0.3%
Probability of Infection - Breathing	0.5%	0.3%	0.2%	0.0%
Net Probability of Infection	96.2%	84.3%	72.5%	17.0%
Number of Additional Infected	58	51	43	10
Normalized Error	7.9%	-4.0%	-15.9%	---------

For the estimated ventilation of 334 cfm (567 m^3/hr), the resulting net probability of infection was estimated to be 84.3%, or an estimated 51 additional infected individuals. This is two less than the likely 53 additional choral members infected. Results are also provided for the +/- 50% uncertainty ventilation rates, giving potential numbers of additional infected individuals of 58 and 43 respectively for the low and high ventilation rates. The difference, or error, between the predicted and actual number of additional people infected, normalized by the total number of uninfected people initially present is also provided. This error was normalized using the total number of uninfected people initially present. In addition, for comparison purposes, results are also provided for the design ventilation and recirculated air rates. If the furnace had been running, providing these design rates, the model estimates a net probability of infection of only 17%, or 10 additional people potentially infected.

The results provided in Table 9 are based on a RH of 30%, though it's possible the RH varied from this depending on how much the furnace dried the air out prior to the practice and how rapidly the RH subsequently increased after the furnace was shut off. To account for this, Figure 1 shows the potential number of additional people infected for 20% RH, 30% RH, and 40% RH.

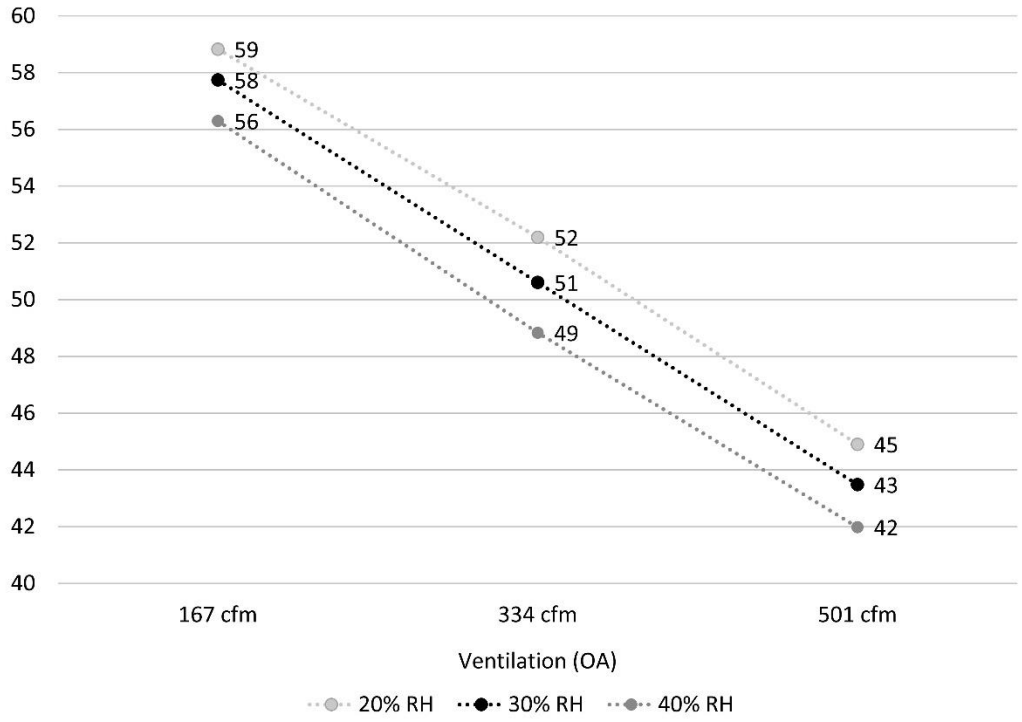

Figure 1: The potential number of additional people infected depending on ventilation and RH.

Depending on the actual choir practice ventilation rate and interior RH (ranging from 20% to 40%), the model's normalized error output ranges in underestimating the probability of infection and resulting number of people potentially infected by 18.4% to overestimating them by 9.7%. If we assume that 334 cfm (567 m^3/hr) is very close to the actual choir practice ventilation rate, then the model's normalized error output ranges in underestimating these values from 6.9% to 1.3%. So overall:

- Normalized error range for all ventilation rates: -18.4% to 9.7%
- Normalized error range for 334 cfm (567 m^3/hr) outside air: -6.9% to -1.3%

Guangzhou restaurant event

On January 24, 2020, a spreading event is thought to have occurred at an unnamed restaurant in Guangzhou, China.[87,88] It occurred on the third floor of the restaurant in question, where a single index case is thought to have infected nine additional patrons out of a total of 89 patrons present for between 53 and 75 minutes. Masks were not worn. Based on the associated epidemiological data, data gathered on the restaurant and its operations, as well as an analysis involving tracer gas and computer simulation, the following parameters were entered into the model.

Dining room size: The estimated area and ceiling heights are taken directly from the referenced analyses.[87,88] Scenario 1 examines the whole third floor dining area. Scenario 2 only looks at the air

conditioning zone within which the infections occurred. No patrons outside of this particular zone ended up being infected. Within the dining room there are five ceiling mounted fan-coil air conditioning units located along one of the long walls, each serving a separate "zone" within the room, with its own supply and return at the unit. While there are no physical barriers between the zones to prevent air mixing across the zones, the air flow from the supply out across the width of the room and then back to the return does limit some of the mixing. In addition, the zone in which the infections occurred was also at the far end of the room, further isolating it from the other zones. As this model assumes droplets / aerosols are instantaneously, continuously, and evenly distributed throughout the room upon expiration, applying it to the whole dining space may be too great a simplification to accurately predict the probability of infection given the limitations on air mixing between the zones. Therefore, an analysis is also run on the one zone only where the infections occurred. This results in the two scenarios being analysed.

- Scenario 1: 1,482.2 ft^2 (137.7 m^2), 10.3 ft (3.14 m) ceiling.
- Scenario 2: 193.8 ft^2 (18 m^2), 10.3 ft (3.14 m) ceiling.

Ventilation OA: Ventilation in the space was apparently limited to brief, infrequent openings of the fire door and infiltration due to negative air pressure created by the restroom exhaust fan running.[88] While the dining space had wall mounted exhaust fans to promote ventilation they were turned off during the period in question. And the five fan-coil air conditioning units serving the dining space did not supply outdoor air - they are recirculating only units. Based on the tracer gas analysis,[88] the air changes per hour (ACH) during the period in question was estimated to be between 0.56 and 0.77. These values along with the volume of the dining space for each scenario were used to determine the following cfm ranges.

- Scenario 1: 142 cfm (242 m^3/hr) - 196 cfm (333 m^3/hr)
- Scenario 2: 18.6 cfm (31.7 m^3/hr) - 25.6 cfm (43.5 m^3/hr)

Recirculated air (RA): Unfortunately, no detailed information on the fan-coil air conditioning units was provided. Based on the image in a letter response from one of the analyses,[89] these appear to be cassette fan-coil units in a chilled water DX split system. To estimate the recirculated air supplied by each unit, a design ventilation rate was first estimated using ASHRAE 62.1. Based on the square footage of the dining space, this rate is determined to be 1,045 cfm (1,776 m^3/hr) for the whole dining area. A rough rule of thumb is that ventilation air is 20% of the total supply air. As the recirculated air is total supply air minus ventilation air, RA is then estimated at 4,180 cfm (7,102 m^3/hr) using this rule of thumb.

The ESACIR horizontal concealed ceiling exposed cassette chilled water fan coil unit, by Shenzhen Eurostars Technology Co., Ltd.,[90] is likely similar to the fan coil unit depicted in the image referenced above.[89] From the drawings/plans in one of the referenced analyses,[88] there may have been two different sizes of units. Using the listed high air flow ratings for a 2-pipe system, (3) of the 1000HC2 units (1,000 cfm / 1,700 m^3/hr) and (2) of the 600HC2 units (600 cfm / 1,020 m^3/hr) would satisfy the RA calculated above. As the speed these units were likely running at was not reported, the medium speed/airflow setting was decided for this analysis. And per the above drawings/plans, the air-flow zone where the infections occurred was served by one of the larger units. Therefore, the RA is estimated to be as follows for each scenario:

- Scenario 1: 3,161 cfm (5,370 m^3/hr)

- Scenario 2: 753 cfm (1,280 m^3/hr)

Fan coil unit filter: MERV 4 for both scenarios. For the ESACIR unit mentioned above, a washable filter is listed as optional. Such filters typically have a MERV rating of 1 to 4. Other similar cassette fan coil units may accept disposable filters ranging in MERV ratings from 1 to 13, though ratings above 4 typically require the addition of a filter box. It doesn't appear in the image[89] referenced above that a filter box is included with the unit, so it is unlikely a filter with a MERV rating greater than 4 was present. As a result of field measurements and computer simulations, the study[88] reported a filtration efficiency of 20% for an aerosol diameter of 5 µm, which would suggest the presence of a MERV 4 or equivalent filter.[9,8] Each scenario is therefore run using a MERV 4 filter.

Temperature: No information was given on the interior temperature in any of the referenced analyses.[87,88,89] The interior temperature was assumed within the 68^{O}F - 76^{O}F (20^{O}C - 24.4^{O}C) that this model is currently optimized for.

Relative humidity (RH): 40% RH for both scenarios. No information was given on the RH in any of the referenced analyses.[87,88,89] As the air conditioning fan coil units were running with very little outside air provided, the RH humidity was assumed to have been lower than the exterior average 72% RH for this time of year in Guangzhou, somewhere between 30% and 50%. While the analysis could have been run for 30%, 40%, and 50%, based on the limited impact of RH within a similar range on the previous Skagit Valley chorale superspreading event analysis, it was decided to focus only on 40% RH to simplify the analysis.

Number of infected individuals: One for both scenarios. As reported in the referenced analyses, [87,88] one infected individual sitting at the middle table of the air-flow zone in which all of the infections occurred served as the infected person.

Viral shedding level: High for both scenarios. This person was reported to have developed symptoms later that day, so this person appears to have been pre-symptomatic while dining in the restaurant. It has been reported that patients may be most infectious in the initial period after infection, before or shortly after symptoms emerge.[91,92,93] For these reasons, the authors of the study[88] estimated that the index case had a "relative large quanta generation rate" while dining. This study followed their lead and used the high shedder condition for the index case.

Activity level: Light. Sitting while talking and eating would be more along the lines of office work as opposed to passively sitting while resting. Therefore a "light" activity level was selected.

Number of patrons present: For the purposes of this analysis, waiters and other restaurant staff are excluded from the analysis, as they were not consistently present within the dining area. The study[88] reported 89 patrons were present during the time in question, and that 21 patrons sat within the airflow zone in which the infections occurred. In addition, nine patrons were infected as a result of this incident, all sitting at the tables encompassed within Scenario 2. No indication of adults versus children among the patrons was provided so it is assumed these are all adults. Therefore, the number of patrons for each scenario consists as follows:

- Scenario 1: 89 patrons, including the single infected person and the nine additional infected individuals.

- Scenario 2: 21 patrons, including the single infected person and the nine additional infected individuals.

Expiratory means / exposure time: The following breakdown was selected for this analysis. The probability of infection was calculated for each time period and the net probability of infection determined from these three individual values.

- Speaking Loudly: 6 minutes (0.1 hours)
- Speaking: 24 minutes (0.4 hours)
- Breathing (Listening/Eating/Drinking): 36 minutes (0.6 hours)

The time of exposure reported in the referenced analyses[87,88] was only for the three tables located in the airflow zone in which the infections occurred. Three families occupied these three tables at the following times - Table A: 12:01 - 13:23, Table B: 11:37 - 12:54, and Table C: 12:03 - 13:18. The infected person sat at Table A, overlapping with Table B by 53 minutes and with Table C by 75 minutes. Averaging the (2) times together results in 64 minutes, which is rounded up to 66 minutes to equate to an even 1.1 hours of exposure time. The amount of time Table A overlapped with the remaining 68 patrons is unknown, so 1.1 hours is used as an approximation.

Little information in the referenced analyses[87,88] is provided on the expiratory means, and these patrons were assumed to have spent their time in the restaurant breathing, eating/drinking, speaking, and potentially speaking loudly. For the purposes of this analysis, breathing is assumed to expel a similar quantity and size distribution of virus-containing aerosols as eating/drinking, though this may underestimate the amount produced. Little research in general appears to exist quantifying the amount of a group mealtime spent eating/drinking vs speaking vs listening/breathing.

For the 66 minutes, it is assumed that 24 minutes are spent speaking/listening and waiting for the food to be served, 30 minutes are spent eating/drinking and speaking/listening, and 12 minutes are spent speaking/listening after eating (see Figure 2). For the combined 36 minutes spent just speaking and listening/breathing, it is assumed that 18 minutes are spent speaking and 18 minutes are spent listening/breathing. And 6 of the 18 minutes is assumed to be spent speaking more loudly. For the 30 minutes spent eating/drinking and speaking/listening, it is assumed that 18 minutes are spent eating/drinking/breathing and listening/breathing and 12 minutes spent speaking.

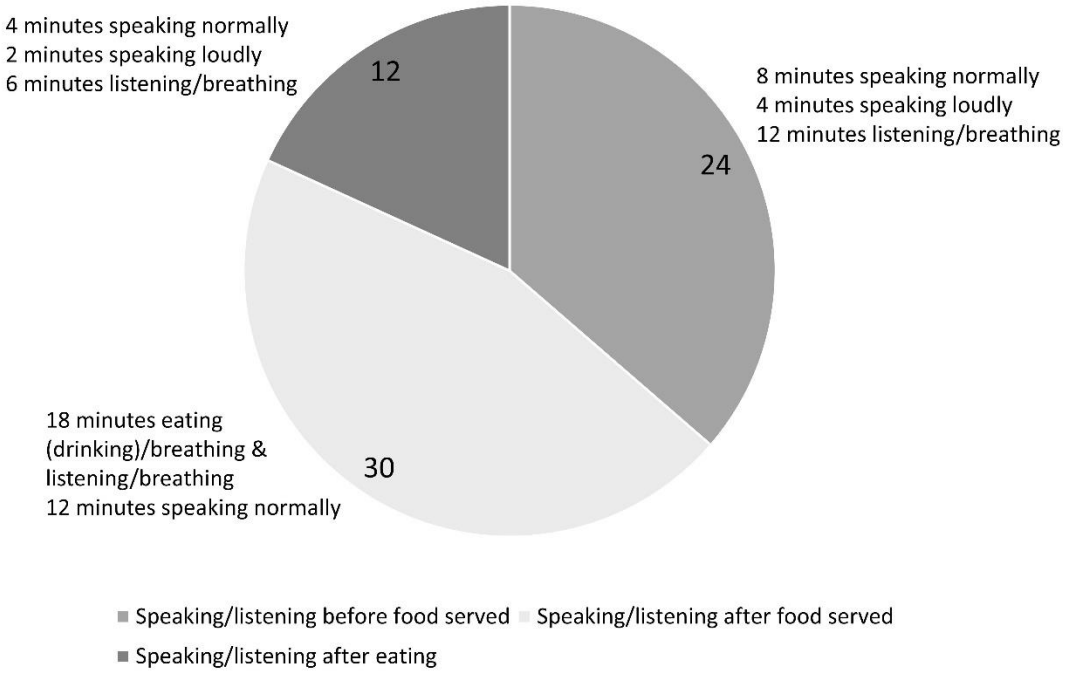

Figure 2: Expiratory means / exposure time (in minutes) estimations for the Guangzhou restaurant event analysis

Table 10 provides a) the resulting probability of infections and b) the potential number of additional people infected given the net probability of infection. The probability of infection for the three different expiratory means / exposure times are listed as well as the resulting net probability (the chance that at least one of these three conditions occurs). The number of additional people infected is the net probability of infection multiplied by 88 uninfected individuals (for scenario 1) and 20 uninfected individuals (for scenario 2).

Table 10: Probability of infections and resulting additional patrons potentially infected

Scenario	Scenario 1 - Whole Restaurant		Scenario 2 - Airflow Zone of Infection	
Ventilation	142 cfm (242 m^3/hr)	196 cfm (333 m^3/hr)	18.6 cfm (31.7 m^3/hr)	25.6 cfm (43.5 m^3/hr)
MERV Filter Level	4	4	4	4
Virus Shedding Level	High	High	High	High

Probability of Infection - Speaking Loudly	6.0%	5.4%	26.4%	25.0%
Probability of Infection - Speaking	2.9%	2.7%	13.7%	13.0%
Probability of Infection - Breathing	1.2%	1.1%	5.9%	5.6%
Net Probability of Infection	9.8%	9.0%	40.2%	38.4%
Number of Additional Infected	9	8	8	8
Normalized Error: 9 More Infected	-0.4%	-1.3%	-4.8%	-6.6%

If the estimations are generally correct, then for scenario 1 the model's normalized error output ranges from -1.3% to -0.4%, underestimating the number of resulting people infected by one or accurately estimating it, depending on the ventilation rates, given the total number of uninfected patrons present in the room. For scenario 2 the model's normalized error output ranges from -6.6% to -4.8% underestimating the number of additional people by one for both ventilation rates, given the total number of uninfected patrons present in this zone. So overall:

- Scenario 1 Normalized Error Range: -1.3% to -0.4%
- Scenario 2 Normalized Error Range: -6.6% to -4.8%

Interestingly, the model's estimated number of people potentially infected was close to the actual number of patrons infected for both scenarios. As discussed above, the air circulation created by each fan coil unit limited the flow of aerosols across airflow zones, contributing to the resulting additional infections only occurring within the single airflow zone with the index case. That would suggest this model, which assumes aerosols are instantaneously, continuously, and evenly distributed throughout the space being analysed, should be better aligned with scenario 2 than scenario 1. The probability of infections for scenario 2 should better reflect the actual conditions for that airflow zone than the probability of infections for scenario 1 reflect the actual conditions for the entire space.

If this is the case, the fact that the model's analysis of scenario 1 produced results closely aligned with the actual range of additional individuals infected is likely a coincidence partially driven by the number of patrons present in this case study. For example, instead of 20 uninfected patrons in scenario 2, assume nine uninfected patrons were actually present. Then the resulting potential number of additional patrons infected would be three at 25.6 cfm (43.5 m^3/hr) of ventilation. For scenario 1, using 77 uninfected patrons for the whole dining space (11 subtracted from 88), the resulting potential number of additional people infected would be seven at 196 cfm (333 m^3/hr) of ventilation. In this case there is a greater difference between the two scenarios, and scenario 2 likely represents the more accurate assessment of the model's capabilities.

Limitations

There are a number of limitations associated with the model itself, as well as the efforts to validate it. Looking specifically at the model's major limitations, it estimates the probability of infection from airborne transmission only, excluding other routes of transmission such as fomite and direct contact. In addition, the model assumes that the virus-containing aerosols are evenly distributed throughout the space immediately after leaving an infected individual and that the room is a well-mixed condition, with the resulting probability of infection representing an average across the room or space being analysed. It is therefore most applicable for assessing the risk from far-field virus-containing aerosols; it underestimates the risk from near-field virus-containing aerosols that occur at a greater density than the far-field aerosols.

In addition, the quantum generation rates are estimates for many of the listed activity levels and degree of shedding, particularly relative to SARS-CoV-2. As more research is conducted, these values will need to be updated based on what is learned. In addition, due to conflicting data and opinions in the research relative to varying quantum generation rates between adults and children,[11,12] the model currently assumes the same rate for both children and adults.

While the model provides the ability to account for more than one infected individual, it does not allow the user to vary the expiratory means, activity level, quantum of infection, pulmonary ventilation rate, or child versus adult among the infected individuals. The same is generally true for the susceptible individuals, with a few exceptions focused on age.

The model does allow one to differentiate between children and adults for the susceptible individuals, but this distinction is limited to two categories: those less than 18 years of age and those 18 and over. Further variation relative to such factors as pulmonary ventilation (breathing), vaccination rates, etc. are found within each of these two broad categories that are currently not accounted for.

The model does not currently allow one to modify temperature, and it is optimized for interior temperatures between 68^{O}F - 76^{O}F (20^{O}C - 24.4^{O}C). Applying it to other temperature conditions will decrease the model's accuracy. Future versions will look at incorporating the ability to modify temperature. Mask selections are also limited to the 13 types listed in Table 5.

It may be necessary to consult with various experts, such as consulting engineers, commissioning agents, TAB consultants, and/or manufacturers, to verify the most appropriate values to use for such inputs as ventilation rate, recirculated air rate, filter rating, the portable air cleaner's CADR rating, RH, and the upper room UVGI system's upper zone average irradiance or fluency value.

In addition to hinging on using the most appropriate value for the upper room UVGI system's upper zone average irradiance or fluency, the associated upper room UVGI system removal factor calculation is also dependent on the actual room conditions being well-mixed. Conditions of stagnation or high ACH will decrease the accuracy of the results. Future versions will look at improving the incorporation of the impacts of air flow. And at this point there are no known studies linking the susceptibility parameter (Z) for SARS-CoV-2 to RH. As future research illuminates this relationship, the model will need to be updated accordingly.

Vaccine efficacy relative to preventing COVID-19 is still being assessed and the associated adjusted vaccination factor will need to be updated as our understanding of efficacy improves. Nor does the

model account for any immunity generated through previous community infections. In those cases where a large number of such individuals (who are also unvaccinated) may be present within a building population, the results will overestimate the probability of infection to an unknown degree.

Despite these limitations, we have found the model quite useful in evaluating the relative impacts that different mitigation strategies included in the model have on reducing the risk of infection from SARS-CoV-2 and influenza via an airborne transmission route.

Turning to the validation exercises, in general there are a limited number of documented real-world events, or even controlled laboratory experiments, available for use to validate the model. For those that do exist, many of the parameters needed for the inputs of the model have not been recorded and are difficult to estimate (if estimating can be done at all). The studies for the two events selected have either verified or estimated most of the necessary inputs for this model and appear to have provided the best opportunity to validate the model using actual events. That being said, each event comes with its own set of limitations discussed below.

Skagit Valley choral superspreading event

The only estimation made that was not justified by information given in the referenced study[21] itself was the 30% input value used for RH. As discussed above, the study did not provide any estimate of the rehearsal hall room's RH during the event. As the heater had been running immediately prior to the choral practice, the interior humidity was estimated to be lower than 50% and the analysis was run for values of 20% RH, 30% RH, and 40% RH. Note that the results do not vary significantly between these three RH percentages.

The expiratory means / exposure time input values were based directly on the information provided in the study and are discussed in detail above. However, the simplification made with respect to treating the phase 2 portion of the practice similar to the phase 1 portion could have some minimal impact on the results. This and the uncertainty regarding RH are the two weakest links in this analysis. The measurements and estimates made for the rehearsal hall room size, choir practice OA and RA, the interior temperature, number of infected individuals, viral shedding level, activity level, number of choral members present, and the number of resulting choral members infected are discussed in detail in the referenced study. These estimates have generally been well justified by the authors of this study.

Guangzhou restaurant event

Estimates had to be made for recirculated air, temperature, and RH with little justification given by the information in the referenced analyses.[87,88,89] The justification for recirculated air and RH were provided in detail above. There is little justification available for the assumption that the temperature fell within the range optimized for this model. It, along with assigning exposure times to specific expiratory means discussed below, represent the weakest links relative to justifications.

The expiratory means / exposure time input values were based directly on the information provided in the referenced analyses and are discussed in detail above. However, there was little to go on to assign specific exposure times to each expiratory method, relying primarily on the authors' own experiences. If actual times varied significantly from what was assumed, it could have a noticeable impact on the results. The measurements and estimates made for the dining room size, ventilation OA, fan coil unit filter, number of infected individuals, viral shedding level, activity level, number of patrons present, and

resulting number of patrons infected are discussed in detail in the referenced analyses. And these estimates have been well justified by the authors of these analyses.

One of the largest questions posed by running an analysis of the Guangzhou restaurant event relative to the model's assumptions was whether to focus on the entire third floor dining area or only on the single airflow zone with the index case. The latter was likely a closer approximation to a well-mixed environment than the former, and the results of the analysis appeared to support the notion that model applications suffer if the actual environment deviates significantly from well-mixed conditions.

While there are limitations relative to the certainty of some of the inputs for these two events, in the authors' opinions, they nevertheless validate the generally applicability of the model if its major assumptions are closely met. However, there are several other aspects of the model that still require testing if appropriate documented real-world events or controlled laboratory experiments are found. These include validating the model's treatment of portable air cleaners, upper room UVGI systems, mask wearing, vaccination, children, and the quanta estimates for influenza.

Conclusion

At the beginning of the pandemic in early 2020, there was an expressed need from various building owners, facility managers, occupants, and AEC industry consultants to help evaluate the relative contribution of different interior COVID-19 risk mitigation strategies. There was a lack of easily accessible tools and other resources for comparing and ranking different solutions (e.g., increased ventilation, filtration, mask wearing, de-densifying, UV technologies, etc.) for a given context based on both removal efficiency and the probability of infection. This web application[1] and its underlying model were developed specifically to contextually compare and rank available influenza and SARS-CoV-2 mitigation strategies for making our built environments safer.

In this paper, the authors have provided a detailed overview of the underlying model's removal and inactivation mechanisms and its specific model of infection, including required inputs, associated assumptions and their justifications as well as the associated limitations. The model was also validated against two documented spreading events to assess its effectiveness, with the normalized errors for both analyses as follows:

- Skagit Valley Chorale Normalized Error Range for all Ventilation Rates: -18.4% to +9.7%
- Skagit Valley Chorale Normalized Error Range for 334 cfm (567 m^3/hr) Outside Air: -6.9% to -1.3%
- Guangzhou Restaurant Normalized Error Range for Scenario 2: -6.6% to -4.8%

For conditions that generally meet the constraints of the model, these two analyses suggest that the error between modelled and actual number of additional people infected, normalized by the number of uninfected people present, will range from roughly -18.4% to +9.7%. The more certain one can be regarding the input parameters (such as ventilation rates), the smaller these normalized errors will likely be, potentially under 2% as indicated in looking at the range above for the most likely Skagit Valley ventilation rate of 334 cfm (567 m^3/hr). In addition, the farther actual conditions vary from a box configuration, from an instantaneous, continuous, and even distribution of aerosols, and/or from a temperature range of 68^{O}F - 76^{O}F (20^{O}C - 24.4^{O}C), the less applicable this model will be to analysing those conditions.

This suggests the model is appropriate to use when its limitations are adequately accounted for and input parameters can be accurately determined. Design team members, commissioning agents, building owners, or facility managers attempting to use this tool to assess existing buildings or new designs have a much larger potential to accurately verify input parameters compared to modelling past events, some of which occurred in other countries. The results of such analyses are then more likely to have less errors than the results presented here.

But additional validation of the Facility Infection Risk Estimator™[1] and its underlying model against events including other parameters would be useful. Events involving children or children and adults, varying degrees of mask wearing, activity levels other than light, portable filter units, upper room UVGI systems, and influenza instead of SARS-CoV-2 would provide further useful validation. In addition to looking for other events to analyse, the model could also be validated against the monitored effectiveness of mitigation strategies that have been implemented. Opportunities for further development of the model include parameters for SARS-CoV-2 variants, updated data on COVID-19 vaccinations, updated research on masks, updated research on SARS-CoV-2 quanta generation rates, as well as similar updated data/research on influenza.

Authors' contributions

Dr. Marcel Harmon was primarily responsible for the development and implementation of the Facility Infection Risk Estimator™. Dr. Josephine Lau provided reviews, comments, and suggestions for earlier versions of the web application tool and underlying model. Dr. Harmon wrote the paper with Dr. Lau.

Acknowledgements

The authors would like to acknowledge the devotion of resources and time for the development of this freely accessible web application tool by Branchpattern. This includes the time and expertise of several BranchPattern employees to review, beta test, and help implement, including Principals Rick Maniktala and Pete Jefferson, Associate Principal Stuart Shell, and Senior Associate Dannie DiIonno. Stuart Shell also provided reviews of the paper.

Declaration of conflicting interests

Dr. Josephine Lau was paid a small fee by BranchPattern, the firm employing Dr. Marcel Harmon and the owner of the Facility Infection Risk Estimator™, to review and comment on an earlier version of the web application tool. Dr. Lau is also a member of this journal's editorial board but was not involved in the review or decision-making process on the journal's side. The authors declare no other potential conflicts of interest with respect to the research, authorship, and/or publication of this article.

References

1. BranchPattern. Facility Infection Risk Estimator v2.1, https://branchpattern.com/research/facility-infection-risk-estimator/ (2020, accessed 22 March 2021).

2. Greenhalgh T, Jimenez JL, Prather KA, Tufekci Z, Fisman D, Schooley R. Ten scientific reasons in support of airborne transmission of SARS-CoV-2. *Lancet* 2021; 397: 1603–1605.

3. Yang W, Elankumaran S, Marr LC. Concentrations and size distributions of airborne influenza A viruses measured indoors at a health centre, a day-care centre and on aeroplanes. *J R Soc Interface* 2011; 8: 1176–1184.

4. Smieszek T, Lazzari G, Salathé M. Assessing the Dynamics and Control of Droplet- and Aerosol-Transmitted Influenza Using an Indoor Positioning System. *Sci Rep* 2019; 9: 2185.

5. Ladhani L, Pardon G, Meeuws H, van Wesenbeeck L, Schmidt K, Stuyver L, van der Wijngaart W. Sampling and detection of airborne influenza virus towards point-of-care applications. *PLoS One* 2017; 12: e0174314.

6. Randall K, Ewing ET, Marr L, Jimenez J, Bourouiba L. How Did We Get Here: What Are Droplets and Aerosols and How Far Do They Go? A Historical Perspective on the Transmission of Respiratory Infectious Diseases, https://papers.ssrn.com/abstract=3829873 (2021, accessed 1 June 2021).

7. Allen JG, Ibrahim AM. Indoor Air Changes and Potential Implications for SARS-CoV-2 Transmission. *JAMA* 2021; 325: 2112–2113.

8. Azimi P, Stephens B. HVAC filtration for controlling infectious airborne disease transmission in indoor environments: Predicting risk reductions and operational costs. *Build Environ* 2013; 70: 150–160.

9. Stephens B. *Wells-Riley & HVAC Filtration for infectious airborne aerosols NAFA Foundation Report HVAC filtration and the Wells-Riley approach to assessing risks of infectious airborne diseases Final Report Prepared for: The National Air Filtration Association (NAFA)*. Virginia Beach, VA, www.built-envi.com (2012, accessed 10 March 2021).

10. Mikszewski A, Buonanno G, Stabile L, Pacitto A. *Airborne Infection Risk Calculator User's Manual*, https://cires.colorado.edu/news/covid-19-airborne-transmission-tool-available (2020, accessed 9 March 2021).

11. Chen SC, Liao C-M. Modelling control measures to reduce the impact of pandemic influenza among schoolchildren. *Epidemiol Infect* 2008; 136: 1035–1045.

12. Jimenez JL. 2020_COVID-19_Aerosol_Transmission_Estimator - Google Sheets, v. 3.4.22, https://docs.google.com/spreadsheets/d/16K1OQkLD4BjgBdO8ePj6ytf-RpPMlJ6aXFg3PrIQBbQ/edit#gid=519189277 (2020, accessed 9 March 2021).

13. Rudnick SN, Milton DK. Risk of indoor airborne infection transmission estimated from carbon dioxide concentration. *Indoor Air* 2003; 13: 237–245.

14. Fabian MP, McDevitt JJ, DeHaan WH, Fung ROP, Cowling BJ, Chan K-H, Leung GM, Milton DK. Influenza Virus in Human Exhaled Breath: An Observational Study. *PLoS One* 2008; 3: e2691.

15. Zemouri C, Awad SF, Volgenant CMC, Crielaard W, Laheij AMGA, de Soet JJ. Modeling of the Transmission of Coronaviruses, Measles Virus, Influenza Virus, Mycobacterium tuberculosis, and Legionella pneumophila in Dental Clinics. *J Dent Res* 2020; 99: 1192–1198.

16. Beggs CB, Avital EJ. Upper-room ultraviolet air disinfection might help to reduce COVID-19 transmission in buildings. *medRxiv* 2020; 2020.06.12.20129254.

17. Bueno de Mesquita PJ, Noakes CJ, Milton DK. Quantitative aerobiologic analysis of an influenza human challenge-transmission trial. *Indoor Air* 2020; 30: 1189–1198.

18. Liao C-M, Chen SC, Chang CF. Modelling respiratory infection control measure effects. *Epidemiol Infect* 2008; 136: 299–308.

19. Buonanno G, Morawska L, Stabile L. Quantitative assessment of the risk of airborne transmission of SARS-CoV-2 infection: Prospective and retrospective applications. *Environ Int* 2020; 145: 106112.

20. Buonanno G, Stabile L, Morawska L. Estimation of airborne viral emission: Quanta emission rate of SARS-CoV-2 for infection risk assessment. *Environ Int* 2020; 141: 105794.

21. Miller SL, Nazaroff WW, Jimenez JL, Boerstra A, Buonanno G, Dancer SJ, Kurnitski J, Marr L, Morawska L, Noakes CJ. Transmission of SARS-CoV-2 by inhalation of respiratory aerosol in the Skagit Valley Chorale superspreading event. *medRxiv* 2020; 2020.06.15.20132027.

22. Dai H, Zhao B. Association of infected probability of COVID-19 with ventilation rates in confined spaces: a Wells-Riley equation based investigation. *medRxiv* 2020; 2020.04.21.20072397.

23. U.S. EPA (Environmental Protection Agency). *Exposure Factors Handbook 2011 Edition (Final Report)*. Washington, DC, https://cfpub.epa.gov/ncea/risk/recordisplay.cfm?deid=236252 (2011, accessed 10 March 2021).

24. Gammaitoni L, Nucci MC. Using a mathematical model to evaluate the efficacy of TB control measures. *Emerg Infect Dis* 1997; 3: 335–342.

25. Marr LC, Tang JW, Van Mullekom J, Lakdawala, SS. Mechanistic insights into the effect of humidity on airborne influenza virus survival, transmission and incidence. *J R Soc Interface* 2019; 16: 20180298.

26. de Oliveira PM, Mesquita LCC, Gkantonas S, Giusti A, Mastorakos E. Evolution of spray and aerosol from respiratory releases: theoretical estimates for insight on viral transmission. *medRxiv* 2020; 2020.07.23.20160648.

27. Yang W, Marr LC. Mechanisms by which ambient humidity may affect viruses in aerosols. *Appl Environ Microbiol* 2012; 78: 6781–6788.

28. Evans P. Properties of Air at atmospheric pressure. *The Engineering Mindset.com*, https://theengineeringmindset.com/properties-of-air-at-atmospheric-pressure/ (2015, accessed 10 March 2021).

29. Fabian MP, Brain J, Houseman EA, Gern J, Milton DK. Origin of exhaled breath particles from healthy and human rhinovirus-infected subjects. *J Aerosol Med Pulm Drug Deliv* 2011; 24: 137–147.

30. Milton DK, Fabian MP, Cowling BJ, Grantham ML, McDevitt JJ. Influenza Virus Aerosols in Human Exhaled Breath: Particle Size, Culturability, and Effect of Surgical Masks. *PLOS Pathog* 2013; 9: e1003205.

31. Morawska L, Johnson GR, Ristovski ZD, Hargreaves M, Mengersen K, Corbett S, Chao CYH, Li Y, Katoshevski, D. Size distribution and sites of origin of droplets expelled from the human respiratory tract during expiratory activities. *J Aerosol Sci* 2009; 40: 256–269.

32. Gregson FKA, Watson NA, Orton CM, Haddrell AE, McCarthy LP, Finnie TJR, Gent N, Donaldson, GC, Shah PL, Calder JD, Bzdek BR, Costello D, Reid JP. Comparing the Respirable Aerosol Concentrations and Particle Size Distributions Generated by Singing, Speaking and Breathing. *ChemRxiv*; 1. Epub ahead of print 20 August 2020. DOI: 10.26434/chemrxiv.12789221.v1.

33. Johnson GR, Morawska L, Ristovski ZD, Hargreaves M, Mengersen K, Chao CYH, Wan MP, Li Y, Xie X, Katoshevski D, Corbett S. Modality of human expired aerosol size distributions. *J Aerosol Sci* 2011; 42: 839–851.

34. Lindsley WG, Blachere FM, Thewlis RE, Vishnu A, Davis KA, Cao G, Palmer JE, Clark KE, Fisher MA, Khakoo R, Beezhold DH. Measurements of Airborne Influenza Virus in Aerosol Particles from Human Coughs. *PLoS One* 2010; 5: e15100.

35. Lindsley WG, Blachere FM, Beezhold DH, Thewlis RE, Noorbakhsh B, Othumpangat S, Goldsmith WT, McMillen CM, Andrew ME, Burrell CN, Noti, JD. Viable influenza A virus in airborne particles expelled during coughs versus exhalations. *Influenza Other Respi Viruses* 2016; 10: 404–413.

36. Han ZY, Weng WG, Huang QY. Characterizations of particle size distribution of the droplets exhaled by sneeze. *J R Soc Interface* 2013; 10: 20130560.

37. Duguid JP. The size and the duration of air-carriage of respiratory droplets and droplet-nuclei. *J Hyg (Lond)* 1946; 44: 471–479.

38. Yang W, Marr LC. Dynamics of Airborne Influenza A Viruses Indoors and Dependence on Humidity. *PLoS One* 2011; 6: e21481.

39. Chia PY, Coleman KK, Tan YK, Milton DK, Gray GC, Schuster S, Barkham T, De PP, Vasoo S, Chan M, Ang BSP, Tan BH, Leo Y-S, Ng O-T, Wong MSY, Marimuthu K, Lye DC, Lim PL, Lee CC, Ling LM, Lee L, Lee TH, Wong CS, Sadarangani S, Lin RJ, Ng DHL, Sadasiv M, Yeo TW, Choy CY, Tan GSE, Dimatatac F, Santos IF, Go CJ, Chan YK, Tay JY, Tan JY-L, Pandit N, Ho BCH, Mendis S, Chen YYC, Abdad MY, Moses D. Detection of air and surface contamination by SARS-CoV-2 in hospital rooms of infected patients. *Nat Commun* 2020; 11: 2800.

40. Fennelly KP. Particle sizes of infectious aerosols: implications for infection control. *Lancet Respir Med* 2020; 8: 914–924.

41. Santarpia JL, Rivera DN, Herrera VL, Morwitzer MJ, Creager HM, Santarpia, GW, Crown KK, Brett-Major DM, Schnaubelt ER, Broadhurst MJ, Lawler JV, Reid SP, Lowe JJ. Aerosol and Surface Transmission Potential of SARS-CoV-2. *medRxiv* 2020; 2020.03.23.20039446.

42. Sharp DG, Taylor AR, McLean Jr. IW, Beard D, Beard JW. Densities and sizes of the Influenza

viruses A (PR8 strain) and B (Lee strain) and the Swine Influenza virus. *J Biol Chem* 1945; 159: 29–44.

43. Stewart EJ, Mead K, Olmsted RN, Pantelic J, Schoen LJ, Sekhar C, Vernon W, Li Y, Sultan ZM, Conian W. *ASHRAE Position Document on Infectious Aerosols*, www.ashrae.org (2020, accessed 8 March 2021).

44. Dietz L, Horve PF, Coil DA, Fretz M, Eisen JA, Van Den Wymelenberg K. 2019 Novel Coronavirus (COVID-19) Pandemic: Built Environment Considerations To Reduce Transmission. *mSystems* 2020; 5: e00245-20.

45. Wargocki P, Kuehn TH, Burroughs HEB, Muller CO, Conrad EA, Saputa, DA, Fisk WJ, Siegel JA, Jackson MC, Veeck A, Francisco P. *ASHRAE Position Document on Filtration and Air Cleaning*, www.ashrae.org (2015, accessed 8 March 2021).

46. Morawska L, Tang JW, Bahnfleth WP, Bluyssen PM, Boerstra A, Buonanno G, Cao J, Dancer SJ, Floto A, Franchimon F, Haworth C, Hogeling J, Isaxon C, Jimenez JL, Kurnitski J, Li Y, Loomans M, Marks Guy, Marr LC, Mazzarella L, Melikov AK, Miller SL, Milton DK, Nazaroff WW, Nielsen PV, Noakes CJ, Peccia J, Querol X, Sekhar C, Seppänen O, Tanabe S, Tellier R, Tham KW, Wargocki P, Wierzbicka A, Yao M. How can airborne transmission of COVID-19 indoors be minimised? *Environ Int* 2020; 142: 105832.

47. Zhang J. Integrating IAQ control strategies to reduce the risk of asymptomatic SARS CoV-2 infections in classrooms and open plan offices. *Sci Technol Built Environ* 2020; 26: 1013–1018.

48. Milton DK, Fabian MP, Cowling BJ, Grantham ML, McDevitt JJ. Influenza Virus Aerosols in Human Exhaled Breath: Particle Size, Culturability, and Effect of Surgical Masks. *PLOS Pathog* 2013; 9: e1003205.

49. Lee J, Yoo D, Ryu S, Ham S, Lee K, Yeo M, Min K, Yoon C. Quantity, Size Distribution, and Characteristics of Cough-generated Aerosol Produced by Patients with an Upper Respiratory Tract Infection. *Aerosol Air Qual Res* 2019; 19: 840–853.

50. Yan J, Grantham ML, Pantelic J, Bueno de Mesquita PJ, Albert B, Liu F, Ehrman S, Milton DK. Infectious virus in exhaled breath of symptomatic seasonal influenza cases from a college community. *Proc Natl Acad Sci* 2018; 115: 1081 LP – 1086.

51. Kirkman S, Zhai J, Miller SL. *Effectiveness of Air Cleaners for Removal of Virus-Containing Respiratory Droplets: Recommendations for Air Cleaner Selection for Campus Spaces*, https://shellym80304.files.wordpress.com/2020/06/air-cleaner-report.pdf (2020, accessed 9 March 2021).

52. Xiaoping L, Jianlei N, Naiping G. Co-occupant's exposure of expiratory droplets—Effects of mouth coverings. *HVAC&R Res* 2012; 18: 575–587.

53. Asadi S, Cappa CD, Barreda S, Wexler AS, Bouvier NM, Ristenpart WD. Efficacy of masks and face coverings in controlling outward aerosol particle emission from expiratory activities. *Sci Rep* 2020; 10: 15665.

54. Clapp PW, Sickbert-Bennett EE, Samet JM, Berntsen J, Zeman KL, Anderson DJ, Weber DJ, Bennett WD. Evaluation of Cloth Masks and Modified Procedure Masks as Personal Protective Equipment for the Public During the COVID-19 Pandemic. *JAMA Intern Med*. Epub ahead of print 10 December 2020. DOI: 10.1001/jamainternmed.2020.8168.

55. Drewnick F, Pikmann J, Fachinger F, Moormann L, Sprang F, Borrmann S. Aerosol filtration efficiency of household materials for homemade face masks: Influence of material properties, particle size, particle electrical charge, face velocity, and leaks. *Aerosol Sci Technol* 2021; 55: 63–79.

56. Konda A, Prakash A, Moss GA, Schmoldt M, Grant GD, Guha S. Aerosol Filtration Efficiency of Common Fabrics Used in Respiratory Cloth Masks. *ACS Nano* 2020; 14: 6339–6347.

57. Konda A, Prakash A, Moss GA, Schmoldt M, Grant, GD, Guha S. Response to Letters to the Editor on Aerosol Filtration Efficiency of Common Fabrics Used in Respiratory Cloth Masks: Revised and Expanded Results. *ACS Nano* 2020; 14: 10764–10770.

58. Mueller A V., Eden MJ, Oakes JM, Bellini C, Fernandez LA. Quantitative Method for Comparative Assessment of Particle Removal Efficiency of Fabric Masks as Alternatives to Standard Surgical Masks for PPE. *Matter* 2020; 3: 950–962.

59. Ueki H, Furusawa Y, Iwatsuki-Horimoto K, Imai M, Kabata H, Nishimura H, Kawaoka Y. Effectiveness of Face Masks in Preventing Airborne Transmission of SARS-CoV-2. *mSphere* 2020; 5: e00637-20.

60. Rothamer DA, Sanders S, Reindl D, Bertram TH. Strategies to minimize SARS-CoV-2 transmission in classroom settings: Combined impacts of ventilation and mask effective filtration efficiency. *medRxiv* 2021; 2020.12.31.20249101.

61. Yang W, Elankumaran S, Marr LC. Relationship between Humidity and Influenza A Viability in Droplets and Implications for Influenza's Seasonality. *PLoS One* 2012; 7: e46789.

62. Lin K, Marr LC. Humidity-Dependent Decay of Viruses, but Not Bacteria, in Aerosols and Droplets Follows Disinfection Kinetics. *Environ Sci Technol* 2020; 54: 1024–1032.

63. Morris DH, Yinda KC, Gamble A, Rossine FW, Huang Q, Bushmaker T, Fischer RJ, Matson MJ, Doremalen, N van, Vikesland PJ, Marr LC, Munster VJ.Lloyd-Smith, James O.. Mechanistic theory predicts the effects of temperature and humidity on inactivation of SARS-CoV-2 and other enveloped viruses. *bioRxiv* 2020; 2020.10.16.341883.

64. DHS (Department of Homeland Security). Estimated Airborne Decay of SARS-CoV-2, https://www.dhs.gov/science-and-technology/sars-airborne-calculator (accessed 8 March 2021).

65. Cabaj A, Jalnik K, Kohmoto K, Levin RE, Nardell EA, Riley RL, van den Beld GJ, Vincent RL. *Ultraviolet Air Disinfection | CIE*, http://cie.co.at/publications/ultraviolet-air-disinfection (2003, accessed 8 March 2021).

66. First MW, Nardell EA, Chaisson W, Riley R. Guidelines for the application of upper-room ultraviolet germicidal irradiation for preventing transmission of airborne contagion -- Part 1:

Basic principles. United States: American Society of Heating, Refrigerating and Air-Conditioning Engineers, Inc., Atlanta, GA (US), https://www.osti.gov/biblio/20002362 (1999).

67. Miller SL, Hernandez M, Fennelly KP, Martyny J, Macher J, Kujundzic E, Xu P, Fabian MP, Peccia J, Howard C. *Efficacy of ultraviolet irradiation in controlling the spread of tuberculosis.* Washington, DC, https://www.cdc.gov/niosh/nioshtic-2/20022472.html (2002, accessed 9 March 2021).

68. First MW, Nardell EA, Chaisson W, Riley R. Guidelines for the application of upper-room ultraviolet germicidal irradiation for preventing transmission of airborne contagion -- Part 2: Design and operation guidance. United States: American Society of Heating, Refrigerating and Air-Conditioning Engineers, Inc., Atlanta, GA (US), https://www.osti.gov/biblio/20002363 (1999).

69. Noakes CJ, Beggs CB, Sleigh A. Modelling the Performance of Upper Room Ultraviolet Germicidal Irradiation Devices in Ventilated Rooms: Comparison of Analytical and CFD Methods. *Indoor Built Environ* 2004; 13: 477–488.

70. Nunayon SS, Zhang H, Lai ACK. Comparison of disinfection performance of UVC-LED and conventional upper-room UVGI systems. *Indoor Air* 2020; 30: 180–191.

71. Su C, Lau J, Gibbs SG. Student absenteeism and the comparisons of two sampling procedures for culturable bioaerosol measurement in classrooms with and without upper room ultraviolet germicidal irradiation devices. *Indoor Built Environ* 2014; 25: 551–562.

72. Kowalski WJ, Walsh TJ, Petraitis V. *2020 COVID-19 Coronavirus Ultraviolet Susceptibility*, https://www.researchgate.net/publication/339887436_2020_COVID-19_Coronavirus_Ultraviolet_Susceptibility (2020, accessed 9 March 2021).

73. Kowalski WJ, Bahnfleth WP, Witham DL, Severin BF, Whittam TS. Mathematical Modeling of Ultraviolet Germicidal Irradiation for Air Disinfection. *Quant Microbiol* 2000; 2: 249–270.

74. McDevitt JJ, Rudnick SN, Radonovich LJ. Aerosol susceptibility of influenza virus to UV-C light. *Appl Environ Microbiol* 2012; 78: 1666–1669.

75. Mphaphlele M, Dharmadhikari AS, Jensen PA, Rudnick SN, van Reenen TH, Pagano MA, Leuschner W, Sears TA, Milonova SP, van der Walt M, Stoltz AC, Weyer K, Nardell EA. Institutional Tuberculosis Transmission. Controlled Trial of Upper Room Ultraviolet Air Disinfection: A Basis for New Dosing Guidelines. *Am J Respir Crit Care Med* 2015; 192: 477–484.

76. Noakes CJ, Beggs CB, Sleigh A. Effect of Room Mixing and Ventilation Strategy on the Performance of Upper Room Ultraviolet Germicidal Irradiation Systems. *IAQ Conf, Tampa, FL,* , March 15-17, 2004, https://www.researchgate.net/publication/268274237_Effect_of_Room_Mixing_and_Ventilation_Strategy_on_the_Performance_of_Upper_Room_Ultraviolet_Germicidal_Irradiation_Systems (2004).

77. Noakes CJ, Khan MAI, Gilkeson CA. Modeling infection risk and energy use of upper-room Ultraviolet Germicidal Irradiation systems in multi-room environments. *Sci Technol Built Environ* 2015; 21: 99–111.

78. Rudnick SN, First MW. Fundamental Factors Affecting Upper-Room Ultraviolet Germicidal Irradiation—Part II. Predicting Effectiveness. *J Occup Environ Hyg* 2007; 4: 352–362.

79. Sung M, Kato S. Estimating the germicidal effect of upper-room UVGI system on exhaled air of patients based on ventilation efficiency. *Build Environ* 2011; 46: 2326–2332.

80. CDC (Centers for Disease Control and Prevention). *Flu Vaccination Coverage, United States, 2018–19 Influenza Season*, https://www.cdc.gov/flu/fluvaxview/coverage-1819estimates.htm?web=1&wdLOR=c419B53C4-1DB7-4877-B9C7-5CFB577A2DF2 (2019, accessed 8 March 2021).

81. Jones JH. *Notes On R0*. Stanford University. 2007.

82. Chen SC, Liao C-M. Cost-effectiveness of influenza control measures: a dynamic transmission model-based analysis. *Epidemiol Infect* 2013; 141: 2581–2594.

83. Branswell H. Comparing three Covid-19 vaccines: Pfizer, Moderna, Johnson & Johnson. *Stat*, https://www.statnews.com/2021/02/02/comparing-the-covid-19-vaccines-developed-by-pfizer-moderna-and-johnson-johnson/ (2021, accessed 16 March 2021).

84. Skowronski DM, De Serres G. Safety and Efficacy of the BNT162b2 mRNA Covid-19 Vaccine Correspondence. *N Engl J Med*. Epub ahead of print 17 February 2021. DOI: 10.1056/NEJMc2036242.

85. Ledford H. J&J's one-shot COVID vaccine offers hope for faster protection. *Nature*. Epub ahead of print 29 January 2021. DOI: 10.1038/d41586-021-00119-7.

86. Callaway E, Mallapaty S. Novavax offers first evidence that COVID vaccines protect people against variants. *Nature* 2021; 590: 17–17.

87. Lu J, Gu J, Li K, Xu C, Su W, Lai Z, Zhou D, Yu, Xu B, Yang Z. COVID-19 Outbreak Associated with Air Conditioning in Restaurant, Guangzhou, China, 2020. *Emerg Infect Dis J* 2020; 26: 1628.

88. Li Y, Qian H, Hang J, Chen X, Cheng P, Ling H, Wang S, Liang P, Li J, Xiao S, Wei J, Liu L, Cowling BJ, Kang M. Probable airborne transmission of SARS-CoV-2 in a poorly ventilated restaurant. *Build Environ* 2021; 196: 107788.

89. Lu J, Yang Z. COVID-19 Outbreak Associated with Air Conditioning in Restaurant, Guangzhou, China, 2020. *Emerg Infect Dis J* 2020; 26: 2789.

90. Made-in-China. Shenzhen Eurostars Technology Co., Ltd. Horizontal Concealed Ceiling Exposed Cassette Chilled Water Fan Coil Unit, https://eurostarschiller.en.made-in-china.com/product/CBDEKsnJfWkZ/China-Horizontal-Concealed-Ceiling-Exposed-Cassette-Chilled-Water-Fan-Coil-Unit.html (accessed 21 March 2021).

91. To KK-W, Tsang OT-Y, Leung W-S, Tam, AR, Wu T-C, Lung DC, Yip CC-Y, Cai J-P, Chan JM-C, Chik TS-H, Lau DP-L, Choi CY-C, Chen L-L, Chan W-M, Chan K-H, Ip JD, Ng AC-K, Poon RW-S, Luo CT, Cheng VC-C, Chan JF-W, Hung IF-N, Chen Z, Chen H, Yuen K-Y. Temporal profiles of viral load in posterior oropharyngeal saliva samples and serum antibody responses during infection by SARS-

CoV-2: an observational cohort study. *Lancet Infect Dis* 2020; 20: 565–574.

92. van Doremalen N, Bushmaker T, Morris DH, Holbrook MG, Gamble A, Williamson BN, Tamin A, Harcourt JL, Thornburg NJ, Gerber SI, Lloyd-Smith JO, de Wit E, Munster VJ. Aerosol and Surface Stability of SARS-CoV-2 as Compared with SARS-CoV-1. *N Engl J Med* 2020; 382: 1564–1567.

93. Zou L, Ruan F, Huang M, Liang L, Huang H, Hong Z, Yu J, Kang M, Song Y, Xia J, Guo Q, Song T, He J, Yen, H-L, Peiris M, Wu J. SARS-CoV-2 Viral Load in Upper Respiratory Specimens of Infected Patients. *N Engl J Med* 2020; 382: 1177–1179.